Src Acts as the Target of Matrine to Inhibit the Proliferation of Cancer Cells by Regulating Phosphorylation Signaling Pathways

Xi Zhang
Huazhong University of Science and Technology
Hui Xu
Huazhong University of Science and Technology
Xiaoyang Bi
Huazhong University of Science and Technology
Guoqing Hou
Huazhong University of Science and Technology
Andong Liu
Huazhong University of Science and Technology
Youyun Zhao
Hubei Provincial Hospital of Traditional Chinese Medicine
Guoping Wang
Huazhong University of Science and Technology
Xuan Cao (caoxuan@hust.edu.cn)
Huazhong University of Science and Technology Tongji Medical College https://orcid.org/0000-0001-9713-4192

Research

Keywords: Targeted therapy, proliferation, matrine, Src, phosphorylation signaling pathways

Posted Date: November 23rd, 2020

DOI: https://doi.org/10.21203/rs.3.rs-111006/v1

Abstract

Background: Identification of accurate targets is essential for a successful development of targeted therapy in cancer. Studies have shown that matrine has antitumor activity against many types of cancers, including lung cancer, breast cancer, liver cancer, pancreatic cancer, ovarian cancer and leukemia, etc. However, the direct target in cancer cells of its anticancer effect has not been identified. The purpose of this study was to find the molecular target of matrine to inhibit the proliferation of cancer cells and explore its mechanism of action.

Methods: The effect of matrine on the proliferation of cancer cells were examined by MTT assay. Pull-down assay with matrine-amino coupling resins (MA beads) and liquid chromatography-mass spectrometry/mass spectrometry (LC-MS/MS) were performed to explore the target of matrine. The target of matrine was further validated by competitive binding assay, cellular thermal shift assay (CETSA) and drug affinity responsive target stability (DARTS). A series of in vitro and in vivo experiments were conducted to reveal the mechanisms by which matrine targeted Src to regulate the downstream signaling pathways of Src in cancer cells.

Results: Herein we showed that matrine inhibited the proliferation of cancer in vitro and in vivo. Pull-down assay with MA beads and LC-MS/MS identified Src as the target of matrine. The findings provided solid evidences that matrine directly bound to Src and Src kinase domain is required for its interaction with matrine and Ala392 in the kinase domain participated in matrine-Src interaction. Intriguingly, matrine was proven to inhibit Src kinase activity in a non-ATP-competitive manner by blocking the autophosphorylation of Tyr419 in Src kinase domain. Matrine down-regulated the phosphorylation levels of MAPK/ERK, JAK2/STAT3 and PI3K/Akt signaling pathways via targeting Src.

Conclusions: Collectively, matrine targeted Src, inhibited its kinase activity and down-regulated its downstream MAPK/ERK, JAK2/STAT3 and PI3K/Akt phosphorylation signaling pathways to inhibit the proliferation of cancer cells.

Background

Cancer is the most common disease and remains a great threat to human health worldwide. As the conventional remedial methods, chemotherapy and radiotherapy showed strong side effects which limit their clinical application [1]. Based on the advantages of specifically killing cancer cells without significant toxicity to normal tissues or cells, molecular targeted therapy has achieved good therapeutic effects in cancer patients during the past decades [2]. Molecular targeted therapy drugs can target specific receptors or kinases and preferentially block the signal pathways, thus inhibiting the cell proliferation and eventually leading to cell death [3–5].

Protein phosphorylation is one of the most common and important post-translational modifications (PTMs), which serves as a mechanism to regulate the activity of enzyme or protein-protein interaction in cellular signal transduction [6, 7]. Protein kinases may catalyze the transfer of a phosphoryl group from

ATP to tyrosine, serine or threonine residue of its substrate proteins. Over-expression or aberrant activation of protein kinases can result in a variety of diseases, such as cancer. Thus, protein kinases are the popular targets for the treatment of cancer [8].

With the virtues of low side toxicity and therapeutic selectivity, some novel natural compounds from medicinal plants have been developed to prevent or treat the occurrence and metastasis of cancer, which presents a compelling tendency for cancer therapy. Matrine is one of the alkaloids isolated from the traditional Chinese medicine *Sophora flavescens* Aiton, exhibiting a wide spectrum of pharmacological activities [9]. Matrine has been widely studied in many kinds of cancers, including lung cancer, breast cancer, liver cancer, gastric carcinoma, pancreatic cancer, ovarian cancer and leukemia. Intensive studies confirmed the anti-tumor mechanisms of matrine, including regulation of phosphorylation of proliferation- and apoptosis-related cell signaling pathways [10, 11]. It has been reported that matrine inhibits cell proliferation of human rhabdomyosarcoma cells via inactivation of the ERK signaling [12]. Matrine can reduce the phosphorylation levels of Janus kinase 2 (JAK2) and signal transducer and activator of transcription 3 (STAT3) and inhibits STAT3-dependent transcriptional activity in human cholangiocarcinoma cells [13], and inhibit the proliferation and invasion of bladder cancer cells through PI3K/AKT signaling pathway [14].

Although the antitumor effects of matrine have been extensively studied, its direct targets and the precise molecular mechanisms that play the anticancer role remain to be elusive. In the present study, we designed and synthesized a novel matrine-amino coupling resin (MA beads) to explore the direct targets of matrine and related cell signaling pathways, and revealed the molecular mechanisms of matrine inhibiting the proliferation of cancer cells, providing strong shoring of foundation for the development of active ingredients of traditional Chinese medicine as novel targeted therapy drugs against cancer.

Materials And Methods

Cell culture

Human colon cancer cell HT-29, human breast cancer cell MCF7, human non-small cell lung cancer cell A549, human pancreatic cancer cell BxPC-3, human ovarian cancer cell SKOV3, human cervical cancer cell HeLa and human embryonic kidney cell HEK-293 were all obtained from the American Type Culture Collection (Manasseh's, VA, USA). Gefitinib-resistant human lung cancer cell PC-9-IR was obtained from Cobioer Biotechnology Co., Ltd. (Nanjing, China). PC-9-IR cells were cultured in RPMI1640 medium containing additional 500 nM Gefitinib (Topscience, T1181) to maintain drug resistance. HT-29 cells were cultured in McCoy's 5A medium, BxPC-3 and SKOV3 cells were grown in RPMI 1640 medium, MCF7, A549, HeLa and HEK-293 cells were maintained in Dulbecco’s modified Eagle’s medium (DMEM) supplemented with 10% fetal bovine serum (FBS) and 1% penicillin and streptomycin. All cells were incubated at 37°C under a humidified 5% CO_2 incubator.

Reagents and antibodies

Matrine and Sophocarpine were purchased from Xi'an Natural Field Bio-Technique Co., Ltd. (Xi'an, China). Matrine was dissolved in phosphate buffer saline (PBS) to a stock concentration of 100 mM. KX2-391 was purchased from Topscience Co., Ltd. (Shanghai, China). Src activator peptide (sc-3052) was purchased from Santa Cruz Biotechnology (Santa Cruz, CA, USA).

Antibody against c-Src (sc-8056) was purchased from Santa Cruz Biotechnology. Antibody against HA (TA180128) was obtained from OriGene Technologies, Inc. (Maryland, USA). Antibodies against GST (#5475), phospho-ERK1/2 (T202/Y204) (#4370), ERK1/2 (#4695), phospho-MEK1/2 (S221) (#2338), MEK1/2 (#9122), phospho-JAK2 (Y1007/1008) (#3771), phospho-STAT3 (#9145), STAT3 (#4904), PI3K (#4292), phospho-Akt (S473) (#4060), Akt (#9272), β-actin (#4970) and GAPDH (#5174) were purchased from Cell Signaling Technology, Inc. (Beverly, MA, USA). Antibody against JAK2 (17670-1-AP) was obtained from Proteintech Group, Inc (Chicago, USA). Antibody against phospho-PI3K (Y607) (ab182651) was purchased from Abcam (Cambridge, MA, USA). Phospho-Src (Tyr419) antibody (AF3162) was obtained from Affinity Biosciences Ltd. (USA). Antibodies against Ki67 (MA5-14520), PCNA (13-3900) were purchased from ThermoFisher Scientific (MA, USA). HRP-conjugated anti-mouse and anti-rabbit secondary antibodies were obtained from Santa Cruz Biotechnology (Santa Cruz, CA, USA).

MTT assay

The effect of matrine on the proliferation of cancer cells, including human colon cancer cell HT-29, human breast cancer cell MCF7, human non-small cell lung cancer cell A549, human pancreatic cancer cell BxPC-3, human ovarian cancer cell SKOV3 and human cervical cancer cell HeLa, were determined by MTT assay. Cells were exposed to matrine at various concentrations (0, 0.5, 1.0, 2.0, 3.0 mg/mL) for the indicated time periods (0, 24, 48, 72 h). The absorbance at 570 nm wavelength was measured using microplate reader (Model 680, Bio-Rad, USA).

Animal studies

BALB/c nude mice, aged 4-6 weeks, weighed 18-22 g, were obtained from the Medical Laboratory Animal Center of Tongji Medical College and maintained in pathogen-free conditions. This study was carried out in accordance with the guidelines approved by the Institutional Animal Care and Use Committee of Tongji Medical College, Huazhong University of Science and Technology, Wuhan, China.

To investigate the effect of matrine on tumor proliferation in vivo, the subcutaneous xenograft tumor models were established. BALB/c nude mice were subcutaneously injected with human non-small cell lung cancer cell A549, human pancreatic cancer cells BxPC-3 and human ovarian cancer cell SKOV3, respectively. The animals were treated with intraperitoneal injection of matrine or normal saline three times a week. Tumor size was measured by using a caliper and was calculated by using the following formula: Volume = 1/2 × (length × width^2). After inoculation, the mice were euthanized for assessing tumor load.

2-Amino-ethoxy-matrine synthesis (P1)

Sophocarpine was dissolved in ethanolamine with sodium metal. The reaction was maintained at 60℃ for 30 h with gentle stirring. The product P1 was purified by column chromatography as a brown solid, yield: 65%. HRMS: calculated, $C_{17}H_{29}N_3O_2$ $[M+H]^+$: 308.23, found 308.2337.

Matrine-amino coupling resin synthesis (MA beads, P3)

2-Amino-ethoxy-matrine was dissolved in coupling buffer. AminoLink® coupling resin (Thermo Fisher Scientific, USA) and cyanoborohydride solution were added to the solution, and the reaction mixture was incubated by end-over-end rocking at 4℃overnight. Washed the resins with wash solution and degassed buffer containing 0.05% sodium azide, and store the matrine-amino coupling resins at 4℃.

Affinity pull-down assay and MS analysis

Cell lysates were harvested and incubated with free amino coupling resins (control beads) or matrine-amino coupling resins (MA beads) at 4℃ with gentle rotation. To disturb the specific interaction between matrine-amino coupling resins and its target, free matrine (MA) was mixed with cell lysates before the binding experiment described above. The beads-bound proteins were separated by sodium dodecyl sulfate-polyacrylamide gel electrophoresis (SDS-PAGE) and visualized by Coomassie brilliant blue staining. The protein-containing band in the gel was excised, followed by in-gel digestion and analysis by liquid chromatography-mass spectrometry/mass spectrometry (LC-MS/MS)
(SpecAlly Life Technology Co., Ltd, Wuhan, China).

Cellular thermal shift assay (CETSA)

Briefly, cell lysates were harvested and equally divided into two tubes for incubation for 3 h at room temperature with matrine or PBS. The lysates were aliquoted and each sample was heated at designated temperatures ranging from 42℃ to 64℃ for 3 min, followed by cooling for 3 min at room temperature. The soluble fractions from precipitates were separated by centrifuging at 13,000 rpm for 25 min and then analyzed by Western blot.

Drug affinity responsive target stability (DARTS)

Cells were lysed in lysis buffer containing 200 mM Na_3VO_4, 1 M NaF and protease inhibitor cocktail (Thermo, Rockford, IL, USA). The lysates were 1:10 diluted with TNC buffer [500 mM Tris·HCl (pH 8.0), 500 mM NaCl, 100 mM $CaCl_2$] and equally divided into two aliquots, then treated with matrine or PBS for 1 h at room temperature. After incubation, samples were digested with pronase (Roche Pharmaceutical Ltd., Switzerland) at room temperature for 30 min, and reactions were ceased by adding the loading buffer. Samples were loaded onto 10% SDS-PAGE gels and analysed by Western blot.

Construction of segmented and mutant plasmids

The cDNA of Src was kindly provided by Dr. Jia-Huai Han (School of Life Sciences, Xiamen University, Xiamen, China). According to the structure and functions of Src, constructs containing SH4, Unique and

SH3 domain (USH3); SH4 and Unique domain (SH4-UD); SH3 domain; SH2 domain and Kinase domain encode amino acids 1-150, 1-85, 86-150, 151-269 and 270-536, respectively. Briefly, the genes of full-length Src and Src fragments (USH3, SH4-UD, SH3, SH2 and Kinase) were amplified and inserted into pcDNA3.1-HA between BamHI and XhoI. The mutant plasmids pcDNA3.1-HA-Kinase-A392G was constructed according to the instructions of Fast Site-Directed Mutagenesis Kit (TIANGEN Biotech Co. Ltd., Beijing, China). The primers are described in Supplementary Table 1.

Construction, expression and purification of recombinant proteins

The genes of full-length Src and Src kinase domain were ligated into the BamHI and NotI sites of pGEX-4T-2, respectively. The GST-Src and GST-Kinase fusion proteins were expressed in the *Escherichia coli* strain BL21, induced by isopropyl 1-thio-β-D-galactopyranoside (IPTG) at 22℃ for 3 h. The fusion proteins were purified from bacterial cell lysates by glutathione-agarose beads. The primers are shown in Supplementary Table 2.

Molecular modeling

Molecular docking study was performed using the Discovery Studio 4.5. The crystal structure of Src kinase domain (1YOJ) was obtained from the Protein Data Bank. Matrine was treated with ligand preparation and minimization model to investigate spatial binding pattern of matrine and Src kinase domain.

Kinase activity assay

The activity of Src kinase was measured according to the instructions of Src kinase activity detection kit (GENMED Scientifics Inc., USA). Cells with matrine treatment were lysed supplemented with protease inhibitor cocktail (Thermo Scientific, Rockford, IL, USA). The activity of Src kinase in cancer cells was quantified at a wavelength of 340 nm by SpectraMax i3x multifunctional microplate reader (Molecular Devices Corporation, CA, USA).

Western blot

Cell lysates were harvested and proteins obtained from cell lysates were equally loaded onto 10% SDS-PAGE gels, electrophoresed and transferred to nitrocellulose membranes. Blocked with 5% nonfat milk, the membranes were incubated with primary antibodies overnight, probed with the appropriate secondary antibodies at room temperature. Detection was performed with an enhanced chemiluminescence detection kit (Thermo Scientific, USA) by ChemiDoc MP Imager (BIO-RAD). Loading was normalized with GAPDH or β-actin.

Immunohistochemistry assay

Tumors and tissues of heart, liver, spleen, lung and kidney in mice were embedded in paraffin, cut into 4 μm sections, and either hematoxylin and eosin (H&E) stained or treated with corresponding antibodies for

immunohistochemistry (IHC) evaluation.

Statistical analysis

All data presented are the mean ± SD from at least three independent experiments. An unpaired Student's t-test was used to evaluate the difference between two different treatments. The differences between multiple groups were analyzed by one-way analysis of variance (ANOVA). $P < 0.05$ was considered to be statistically significant.

Results

Matrine inhibits the proliferation of cancer in vitro and in vivo

The effects of matrine on the proliferation of cancer cells, including human colon cancer cell HT-29, human breast cancer cell MCF7, human non-small cell lung cancer cell A549, human pancreatic cancer cell BxPC-3, human ovarian cancer cell SKOV3 and human cervical cancer cell HeLa, were determined by MTT assay. Each cell line was treated with matrine at concentration of 0, 0.5, 1.0, 2.0 or 3.0 mg/mL for 0, 24, 48 or 72 h. The results showed that matrine inhibited the proliferation of cancer cells in a dose- and time-dependent manner (Fig. 1a, Supplementary Fig. 1a). The optimal concentration of matrine was 2.5, 2.5, 3.0, 3.0, 2.0 and 2.5 mg/mL in HT-29, MCF7, A549, BxPC-3, SKOV3 and HeLa cells, respectively (Supplementary Fig. 1b). To further determine the anti-cancer effects of matrine in vivo, we injected subcutaneously cancer cells, including A549, BxPC-3 or SKOV3 cells into BALB/c nude mice, respectively. After inoculation, the mice were treated with an intraperitoneal injection of matrine or normal saline thrice a week. The results demonstrated that tumor volume, size and weight of mice in matrine group were found to be much smaller than those in normal saline group (Fig. 1b-d). H&E staining indicated that matrine caused necrosis lesions in tumor tissues of mice inoculated with three cancer cells. IHC analysis showed that treatment with matrine resulted in a remarkably smaller proportion of proliferation marker proteins Ki-67 and PCNA positive cancer cells in tumors compared with the control group (Fig. 1e). Moreover, histopathological analysis of heart, liver, spleen, lung and kidney of matrine-treated mice showed no obviously change compared to the control group (Supplementary Fig. 2), which suggested that matrine could be a safe agent to cancer in vivo. All these data demonstrated that matrine inhibited the proliferation of cancer in vitro and in vivo without obvious toxicity.

Src is the potential target of matrine

Above data showed that matrine is a potent inhibitor of cancer growth in vitro and in vivo. Then, we sought to explore the potential targets of matrine that mediate its growth inhibitory capability. Matrine and Sophocarpine are alkaloids extracted from the traditional Chinese medicine *Sophora flavescens* Aiton (Fig. 2a). To explore the potential targets of matrine, we prepared chemical probes for affinity purification. Sophocarpine, the structural analog of matrine, was used to synthetize 13α-(2-amino) ethoxymatrine (P1) (Fig. 2b). High-resolution mass spectrum (HRMS) of P1 was gathered on a Bruker MicroTOF-Q III LC-MS instrument operating in electrospray ionization (ESI) (Supplementary Fig. 3a). As

shown in Fig. 2c, matrine-amino coupling resins (MA beads, P3) were made by coupling reaction of 13α-(2-amino) ethoxymatrine with aminolink coupling resins, which were used to pull down the cellular targets of matrine. In addition, competition assay with matrine-amino coupling resins was carried out by adding matrine during coupling reaction. The proteins retained by MA beads were separated by SDS/PAGE and visualized by Coomassie brilliant blue staining. The results showed that one obvious protein band could be observed between 55 and 70 kDa in the group with MA beads but not in group with control beads. Moreover, this protein band was found much weaker with an excess amount of matrine for competition (Fig. 2d). The band in the gel was excised and identified by LC-MS/MS. Mass spectrometric analysis verified this protein as Src protein (Supplementary Table 1).

To further confirm that Src is the direct target protein of matrine, affinity pull-down assay was performed with matrine-amino coupling resins (MA beads) and matrine. As shown in Fig. 2e, Src protein could be precipitated by MA beads, and increasing amount of matrine competitively inhibited the binding between Src and MA beads in cell lysates and tumor tissue lysates. Meanwhile, recombinant protein GST-Src could also be precipitated by MA beads, and competitively inhibited by addition of matrine in immunoblot and sliver staining assays. Furthermore, DARTS results showed that the presence of matrine partially prevents pronase-mediated digestion of Src. Src protein is mostly digested in the absence of matrine, whereas most of them is undigested in the presence of matrine in cell lysates and tumor tissue lysates. GAPDH was used as a negative control, and it was not affected by matrine (Fig. 2f). As ligand may contribute to the stabilization of its target proteins, CETSA was carried out to confirm the interaction between Src and matrine in vitro. The thermal stability of Src protein in cell lysates (Fig. 2g) and tumor tissue lysates (Fig. 2h) was tested by Western blot at the temperature range of 42-64℃ after exposing to matrine or PBS. The results showed that Src was still obviously detectable at the temperature of 60-64℃ in the group exposed to matrine, but not in the control group. Matrine treatment efficiently protected Src protein from temperature-dependent degradation. The significant shift in melting temperatures of Src protein and hence stabilization upon addition of matrine indicated that matrine directly bound to Src protein (Fig. 2i, j). Overall, these results suggested that Src was the direct target of matrine in cancer cells.

Src kinase domain is required for its interaction with matrine

From the N- to C-terminus, Src contains an SH4 domain, a unique domain, an SH3 domain, an SH2 domain, an SH2-kinase linker, a protein-tyrosine kinase domain, and a regulatory tail (Fig. 3a). Src segmented plasmids, including pcDNA3.1-HA-USH3, pcDNA3.1-HA-SH4-UD, pcDNA3.1-HA-SH3, pcDNA3.1-HA-SH2, pcDNA3.1-HA-Kinase were constructed and overexpressed in HEK-293 cells, respectively. The corresponding cell lysates were incubated with MA beads to determine matrine-binding region of Src, which then were dissociated from the beads by denaturation and were probed with anti-HA. Pull-down assay demonstrated that protein band precipitated by MA beads could be only observed in cell lysates transfected with plasmid pcDNA3.1-HA-Kinase. The results indicated that matrine bound directly to the Src kinase domain, and its ability to interact with other regions of Src was negligible (Fig. 3b). To confirm that matrine may definitely bind to the kinase domain of Src, binding competition assay was conducted using pcDNA3.1-HA-Kinase plasmid and GST-Kinase fusion protein. As shown in Fig. 3c,

Kinase proteins were pulled down by MA beads, which were reduced by adding an excess amount of MA in cells transfected with plasmid pcDNA3.1-HA-Kinase and in GST-Kinase recombinant protein.

To dissect the critical amino acids involved in the interaction between Src and matrine, the molecular docking of matrine with Src kinase domain was predicted by Discovery Studio 4.5 software. 3D molecular dynamics simulation analysis revealed that matrine was embedded in the cleft of the Src kinase domain. Van der Waals forces were also formed between matrine and the residues of kinase domain, including Met343, Ser347, Ile 372, Asp388, Leu389 and Arg390. Conspicuously, a strong hydrogen-bonding interaction existed between matrine and the residue of Ala392. (Fig. 3d, e). Then, Ala-392 in the kinase domain was mutated to Gly to confirm its involvement in matrine-Src interaction. Plasmid pcDNA3.1-HA-Kinase-A392G was constructed and transfected into HEK-293 cells as well as pcDNA3.1-HA-Kinase. Pull-down assay was performed to determine whether matrine binds to mutated kinase domain of Src in the transfected cells using MA beads. The results showed that matrine bound to wild type HA-Kinase, while significantly reduced binding was observed for mutant Kinase-A392G. Moreover, the binding was also attenuated in cell lysates expressing mutant plasmid by addition of MA (Fig. 3f, g). These results suggested that Ala392 in the kinase domain exhibited an important role in matrine-Src interaction.

Matrine is a non-ATP-competitive inhibitor of Src kinase

The tyrosine kinase Src is activated in a large number of human malignancies and plays significant roles in the development of cancers. The biochemical and structural basis for the basal inhibition of Src protein tyrosine kinase activity was largely elucidated at present [15-17]. To investigate the effect of matrine on Src kinase activity, cells were treated with the optimal concentration of matrine, respectively. The results showed that after treated with matrine, the Src kinase activities in cancer cells, including HT-29, MCF7, A549, BxPC-3, SKOV3 and HeLa, were significantly decreased (Fig. 4a). ATP-competitive inhibitors have been developed and some are used in clinical research, whereas their inhibitory activities must be strong enough to compete with endogenous ATP [18, 19]. Moreover, a number of non-ATP-competitive inhibitors have also been reported for kinases [20]. Molecular docking results indicated that both matrine and ATP bound to Src kinase domain (Fig. 4b, c). To investigate the competitive interaction between matrine and ATP, we measured IC50 values of matrine at various ATP concentrations in SKOV3 cells. The dose-response curves of matrine at ATP concentrations of 25, 50 and 100 μM are indistinguishable. The corresponding IC50 values are 1.83 ± 0.57, 2.15 ± 0.34, 2.05 ± 0.63 mg/mL. This verified that matrine is a non-ATP-competitive inhibitor of Src kinase domain (Fig. 4d).

It has been shown that protein tyrosine kinase could selectively catalyze phosphorylation of the tail tyrosine site in Src kinase domain [21]. Dephosphorylation of Y530, binding of SH2 and/or SH3 ligands, and phosphorylation of Y419 of the activation loop may activate the Src kinase [22, 23]. Cancer cells, including HT-29, MCF7, A549, BxPC-3, SKOV3 and HeLa, were exposed to matrine at its optimal concentrations for 24 h, respectively. The phosphorylation level of Src Y419 was detected by immunoblot. The results indicated that matrine obviously decreased the tyrosine 419 phosphorylation level of Src after matrine treatment in cancer cells (Fig. 4e). Considering that Src Ala392 is adjacent to Y419, we

speculated that matrine might block the autophosphorylation of tyrosine 419, resulting in inactivation of Src kinase.

Matrine inhibits phosphorylation signaling pathways in cancer cells

Researches have showed that MEK/ERK signaling pathway plays an important role in regulating cell proliferation, differentiation and apoptosis, thus blocking it can inhibit the proliferation of tumor cells [12]. The expression and phosphorylation levels of MEK1/2 and ERK1/2 in cancer cells were detected by Western blot to evaluate the effect of matrine on MAPK/ERK signaling pathway. The results demonstrated that matrine decreased the phosphorylation levels of ERK1/2 and MEK1/2 in different cancer cells, without change of protein expression (Fig. 5a). The phosphorylation ratios of MEK1/2 and ERK1/2 were significantly reduced in HT-29, MCF7, A549, BxPC-3, SKOV3 and HeLa cells (Fig. 5b). Collectively, the phosphorylation levels of MAPK/ERK signaling pathway in cancer cells were dramatically inhibited by matrine.

The association between the JAK/STAT pathway and tumorigenesis is an important clue of tumor biology. STAT3 is an important transcription factor for gene transcription involved in cell proliferation, differentiation, apoptosis, and angiogenesis in a variety of cells [24]. Sustained activation of STAT3 occurs in many cancers, and can promote tumor growth, survival and progression [25]. To investigate the effect of matrine on JAK2/STAT3 signaling pathway, the optimal concentrations of matrine were applied to treat cancer cells. Immunoblot analysis showed that the phosphorylation levels of JAK2 and STAT3 in cancer cells were down-regulated by matrine (Fig. 5c). The phosphorylation ratios of JAK2 were drastically decreased in HT-29, MCF7 and BxPC-3 cells, and the phosphorylation ratios of JAK2 and STAT3 were obviously reduced in HT-29, MCF7, A549, BxPC-3, SKOV3 and HeLa cells (Fig. 5d). Therefore, matrine could significantly suppress the phosphorylation levels of JAK2/STAT3 signaling pathway in cancer cells.

PI3K/Akt signaling pathway is one of the essential pathways that regulate biological behaviors such as cell proliferation and invasion [26, 27]. Activation of PI3K/Akt pathway is often achieved by its phosphorylation, thus we examined the changes of the phosphorylation levels of PI3K and Akt in cancer cells with matrine treatment. As shown in Fig. 5e, after matrine treatment, the phosphorylation levels of PI3K and Akt in cancer cells were decreased. The phosphorylation ratios of PI3K and Akt were markedly decreased in HT-29, MCF7, A549, BxPC-3, SKOV3 and HeLa cells (Fig. 5f). The results above suggested that matrine significantly inhibited the activation of PI3K/Akt signaling pathway in cancer cells.

Meanwhile, IHC staining was performed to confirm that the phosphorylation levels of MEK1/2, ERK1/2, JAK2, STAT3, PI3K and Akt in tumor tissues of mice inoculated with A549, BxPC-3 and SKOV3 cells, respectively. The results demonstrated that the phosphorylation levels of these proteins were significantly decreased in tumors with matrine treatment compared with the control group (Supplementary Fig. 4).

Matrine regulates phosphorylation signaling pathways via targeting Src

Protein phosphorylation is the most widespread class of post-translational modifications in signal transduction [28]. Src interacts with several protein-tyrosine kinase receptors, such as EGFR, c-Met, PDGFR and IGFR, then participates in pathways regulating cell survival, proliferation and regulation of gene expression [29]. Once activated, Src acts as an upstream regulator of the Ras/MAPK and PI3K/Akt pathways inducing malignant transformation [30, 31]. To further verify that Src is the direct target of matrine in regulating the phosphorylation signaling pathways in cancer cells, Src activator peptide was delivered to cancer cells using a DirectX peptide transfection kit (Panomics). HT-29, MCF7, A549, BxPC-3, SKOV3 and HeLa cells were treated with Src activator or Src inhibitor KX2-391, then exposed to matrine at its optimal concentrations for 24 h, respcetively. The phosphorylation levels of MAPK/ERK, JAK2/STAT3 and PI3K/Akt signaling pathways in cancer cells were examined, respectively. The results demenstrated that Src activator peptide increased and KX2-391 decreased the phosphorylation levels of MEK1/2, ERK1/2, JAK2, STAT3, PI3K and Akt in cancer cells. Their protein phosphorylation levels were further inhibited after exposed to matrine (Fig. 6a-c, Supplementary Fig. 5).

Subsequently, human cervical cancer cell HeLa, gefitinib-resistant human lung cancer cell PC-9-IR (mutant of EGFR, upstream protein of Src kinase) and human pancreatic cancer cell AsPC-1 (mutant of Ras, downstream protein of Src kinase) were transfected with plasmid pcDNA3.1-HA-Src, then treated with matrine or KX2-391, respectively. The phosphorylation levels of MEK1/2, ERK1/2, JAK2, STAT3, PI3K and Akt in cancer cells were detected by Western blot. The results showed that both matrine and KX2-391 could inhibited the phosphorylation levels of these proteins in HeLa cells and EGFR mutant PC-9-IR cells. Consistent with our expectation, Src overexpression may rescue the phosphorylation levels of these proteins, and adding an excess amount of MA may decrease their phosphorylation levels again (Fig. 6d, e). Meanwhile, the protein phosphorylation levels of MEK1/2, ERK1/2, JAK2, STAT3, PI3K and Akt had no significant change by matrine or KX2-391 in Ras mutant AsPC-1 cells, and Src overexpression, matrine, KX2-391 or excess amount of MA had no obvious effect on their phosphorylation levels (Fig. 6f). All these data solidly proved that matrine inhibited the proliferation-related phosphorylation signaling pathways via targeting Src.

Discussion

During the past few decades, unprecedented advances have been made in molecular biology and related technologies, which have greatly enhanced the understanding of pathogenesis of cancer, and then improved the therapy of cancer [32]. Chemotherapy and molecular targeted therapy are the main remedies to inhibit the growth and progression of cancer. Unfortunately, chemotherapeutic drugs showed significant toxicity to the normal cells. As a revolutionary therapy, molecular targeted agent may preferentially kill cancer cells by acting on specific target in them [33]. However, drug resistance is its Achilles's hell because of the mutation of the targeted gene or protein, which causes the targeted agent to be futile within 6 to 12 months. To overcome the shortcomings of chemotherapeutic drugs and molecular targeted agents, it is urgent to develop novel anti-cancer drugs. With the advantages of wide spectrum of pharmacological activities and low side toxicity, the discovery and development of novel natural compounds has become a new hotspot in antitumor research.

Modern pharmacological studies have shown that Kushen has a long history of use for the treatment of tumors, inflammation and other diseases in traditional Chinese medicine [34]. Matrine is an alkaloid isolated from *Sophora flavescens* Aiton, possessing a wide spectrum of biological activities [35]. Many researches have showed that matrine has antitumor effect on various types of cancers [36, 37]. However, its direct targets and molecular mechanisms have not been identified yet. The present study demonstrated that matrine inhibited the proliferation of cancer cells in vitro and in vivo. Meanwhile, matrine-amino coupling resins (MA beads) were prepared and used to pull down the targeted proteins of cancer cells.

Src is a non-receptor tyrosine kinase, and its overexpression or overactivation has been strongly implicated in the development, maintenance and progression of human cancers, which indicates that Src may represent a compelling target for the cancer treatment [38, 39]. In our study, LC-MS/MS analysis identified that Src was the target protein of matrine. Furthermore, it was validated that Src was the direct target of matrine by CETSA and DARTS. Moreover, Src segmented plasmids were constructed and overexpressed in HEK-293 cells, pull-down experiment by matrine-amino coupling resins showed that matrine bound directly to the Src kinase domain. Molecular docking prediction and pull-down assay unveiled that a strong hydrogen-bonding interaction existed between matrine and the residues of Ala392 in Src kinase domain, and it participated in matrine-Src interaction. To date, ten additional kinases with homology to Src have been identified in human genome and collectively are referred to as the Src family kinases (SFKs). Intriguingly, although the proportion is very low comparing with Src protein, Lyn (tyrosine-protein kinase Lyn) was also been identified in the data of LC-MS/MS analysis as shown in Table S3.

Studies have shown that Src can interact with several signaling transduction proteins related to proliferation, such as receptor tyrosine kinases, signal transducers and activators of transcription (STATs), G proteins, the mitogen-activated protein kinase ERK2. Src is the hub of several signaling pathways, including Ras/Raf/ERK1/2, PI3K/Akt, and STAT3, resulting in cell proliferation, survival, invasion, migration and angiogenesis [40, 41]. In this study, the effect of matrine on Src kinase activity in cancer cells was examined. The results indicated that Src kinase activity was inhibited by matrine in a non-ATP-competitive manner, and its phosphorylation levels on tyrosine 419 were also decreased by matrine. Meanwhile, matrine down-regulated the phosphorylation levels of MAPK/ERK, JAK2/STAT3 and PI3K/Akt signaling pathways by targeting Src in cancer cells.

Conclusion

In summary, we first designed and synthesized matrine-amino coupling resins (MA beads), aiming to explore the direct targets of matrine. Our findings demonstrated that Src was the target of matrine in cancer cells, and Src kinase domain was the binding region of matrine. Matrine targeted Src, inhibited its kinase activity and tyrosine phosphorylation to inhibit the proliferation of cancer cells by down-regulating the downstream MAPK/ERK, JAK2/STAT3 and PI3K/Akt phosphorylation signaling pathways (Fig. 7). Therefore, matrine can be used as the leading compound by chemically modifying the structure,

providing strong shoring of foundation for the development of active compounds of traditional Chinese medicine as novel targeted therapy drug against cancer.

Abbreviations

LC-MS/MS: Liquid chromatography-mass spectrometry/mass spectrometry; CETSA: Cellular thermal shift assay; DARTS: Drug affinity responsive target stability; PTMs: Post-translational modifications; DMEM: Dulbecco's modified Eagle's medium; FBS: Fetal bovine serum; PBS: Phosphate buffer saline; SDS-PAGE: Sodium dodecyl sulfate-polyacrylamide gel electrophoresis; IPTG: Isopropyl 1-thio-β-D-galactopyranoside; ANOVA: One-way analysis of variance; SFKs: Src family kinases

Declarations

Acknowledgements

Not applicable.

Authors' contributions

XZ, HX and GQH conducted the experiments; ADL, XYB and JZ participated in the data analysis. XC, GPW and XZ designed the experiments and drafted the manuscript. All authors read and approved the final manuscript.

Funding

This work was supported by the National Natural Science Foundation of China (Nos. 31771541, 81974468, 81770263); the Natural Science Foundation of Hubei Province of China (No.2019CFB734).

Consent for publication

The consent to publish this manuscript has been obtained from all authors.

Competing interests

The authors declare that they have no competing interests.

References

1. Siegel RL, Miller KD, Jemal A. Cancer statistics, 2019. CA Cancer J Clin. 2019;69(1):7–34.
2. Krajewski KM, Braschi-Amirfarzan M, DiPiro PJ, Jagannathan JP, Shinagare AB. Molecular Targeted Therapy in Modern Oncology: Imaging Assessment of Treatment Response and Toxicities. Korean J Radiol. 2017;18(1):28–41.

3. Naoum GE, Morkos M, Kim B, Arafat W. Novel targeted therapies and immunotherapy for advanced thyroid cancers. Mol Cancer. 2018;17(1):51.
4. Polivka J Jr, Janku F. Molecular targets for cancer therapy in the PI3K/AKT/mTOR pathway. Pharmacol Ther. 2014;142(2):164–75.
5. Roberts PJ, Der CJ. Targeting the Raf-MEK-ERK mitogen-activated protein kinase cascade for the treatment of cancer. Oncogene. 2007;26(22):3291–310.
6. Appella E, Anderson CW. Post-translational modifications and activation of p53 by genotoxic stresses. Eur J Biochem. 2001;268(10):2764–72.
7. Radivojac P, Baenziger PH, Kann MG, Mort ME, Hahn MW, Mooney SD. Gain and loss of phosphorylation sites in human cancer. Bioinformatics. 2008;24(14):i241-7.
8. Manning G, Whyte DB, Martinez R, Hunter T, Sudarsanam S. The protein kinase complement of the human genome. Science. 2002;298(5600):1912–34.
9. Huang J, Xu H. Matrine. Bioactivities and Structural Modifications. Curr Top Med Chem. 2016;16(28):3365–78.
10. Liu ZM, Yang XL, Jiang F, Pan YC, Zhang L. Matrine involves in the progression of gastric cancer through inhibiting miR-93-5p and upregulating the expression of target gene AHNAK. J Cell Biochem. 2020;121(3):2467–77.
11. Zhang X, Hou G, Liu A, Xu H, Guan Y, Wu Y, et al. Matrine inhibits the development and progression of ovarian cancer by repressing cancer associated phosphorylation signaling pathways. Cell Death Dis. 2019;10(10):770.
12. Yan P, Huang Z, Zhu J. Matrine inhibits cell proliferation and induces apoptosis of human rhabdomyosarcoma cells via downregulation of the extracellular signal-regulated kinase pathway. Oncol Lett. 2017;14(3):3148–54.
13. Yang N, Han F, Cui H, Huang J, Wang T, Zhou Y, et al. Matrine suppresses proliferation and induces apoptosis in human cholangiocarcinoma cells through suppression of JAK2/STAT3 signaling. Pharmacol Rep. 2015;67(2):388–93.
14. Yang Y, Guo JX, Shao ZQ, Gao JP. Matrine inhibits bladder cancer cell growth and invasion in vitro through PI3K/AKT signaling pathway: An experimental study. Asian Pac J Trop Med. 2017;10(5):515–9.
15. Abram CL, Courtneidge SA. Src family tyrosine kinases and growth factor signaling. Exp Cell Res. 2000;254(1):1–13.
16. Young MA, Gonfloni S, Superti-Furga G, Roux B, Kuriyan J. Dynamic coupling between the SH2 and SH3 domains of c-Src and Hck underlies their inactivation by C-terminal tyrosine phosphorylation. Cell. 2001;105(1):115–26.
17. Wang D, Esselman WJ, Cole PA. Substrate conformational restriction and CD45-catalyzed dephosphorylation of tail tyrosine-phosphorylated Src Protein. J Biol Chem. 2002;277(43):40428–33.

18. Schöffski P. Polo-like kinase (PLK) inhibitors in preclinical and early clinical development in oncology. Oncologist. 2009;14(6):559–70.
19. Strebhardt K. Multifaceted polo-like kinases: drug targets and antitargets for cancer therapy. Nat Rev Drug Discov. 2010;9(8):643–60.
20. Harrison S, Das K, Karim F, Maclean D, Mendel D. Non-ATP-competitive kinase inhibitors - enhancing selectivity through new inhibition strategies. Expert Opin Drug Discov. 2008;3(7):761–74.
21. Farkas A, Szatmári E, Orbók A, Wilhelm I, Wejksza K, Nagyoszi P, et al. Hyperosmotic mannitol induces Src kinase-dependent phosphorylation of beta-catenin in cerebral endothelial cells. J Neurosci Res. 2005;80(6):855–61.
22. Roskoski R Jr. Src protein-tyrosine kinase structure, mechanism, and small molecule inhibitors. Pharmacol Res. 2015;94:9–25.
23. Saad F, Lipton A. SRC kinase inhibition: targeting bone metastases and tumor growth in prostate and breast cancer. Cancer Treat Rev. 2010;36(2):177–84.
24. Junk DJ, Bryson BL, Jackson MW. HiJAK'd Signaling; the STAT3 Paradox in Senescence and Cancer Progression. Cancers (Basel). 2014;6(2):741–55.
25. Xiong A, Yang Z, Shen Y, Zhou J, Shen Q. Transcription Factor STAT3 as a Novel Molecular Target for Cancer Prevention. Cancers (Basel). 2014;6(2):926–57.
26. Peng Y, Li L, Huang M, Duan C, Zhang L, Chen J. Angiogenin interacts with ribonuclease inhibitor regulating PI3K/AKT/mTOR signaling pathway inbladder cancer cells. Cell Signal. 2014;26(12):2782–92.
27. Smolensky D, Rathore K, Cekanova M. Phosphatidylinositol-3-kinase inhibitor induces chemosensitivity to a novel derivative of doxorubicin, AD198 chemotherapy in human bladder cancer cells in vitro. BMC Cancer. 2015;15:927.
28. Manning G, Whyte DB, Martinez R, Hunter T, Sudarsanam S. The protein kinase complement of the human genome. Science. 2002;298(5600):1912–34.
29. Olayioye MA, Badache A, Daly JM, Hynes NE. An essential role for Src kinase in ErbB receptor signaling through the MAPK pathway. Exp Cell Res. 2001;267(1):81–7.
30. Mitra SK, Schlaepfer DD. Integrin-regulated FAK-Src signaling in normal and cancer cells. Curr Opin Cell Biol. 2006;18(5):516–23.
31. Ingley E. Src family kinases: regulation of their activities, levels and identification of new pathways. Biochim Biophys Acta. 2008;1784(1):56–65.
32. Cancer Genome Atlas Research Network. Comprehensive genomic characterization defines human glioblastoma genes and core pathways. Nature. 2008;455(7216):1061–8.
33. Lee YT, Tan YJ, Oon CE. Molecular targeted therapy: Treating cancer with specificity. Eur J Pharmacol. 2018;834:188–96.
34. Wang W, You RL, Qin WJ, Hai LN, Fang MJ, Huang GH, et al. Anti-tumor activities of active ingredients in Compound Kushen Injection. Acta Pharmacol Sin. 2015;36(6):676–9.

35. Zhou H, Xu M, Gao Y, Deng Z, Cao H, Zhang W, et al. Matrine induces caspase-independent program cell death in hepatocellular carcinoma through bid-mediated nuclear translocation of apoptosis inducing factor. Mol Cancer. 2014;13:59.
36. Zhang JQ, Li YM, Liu T, He WT, Chen YT, Chen XH, et al. Antitumor effect of matrine in human hepatoma G2 cells by inducing apoptosis and autophagy. World J Gastroenterol. 2010;16(34):4281–90.
37. Zhang L, Wang T, Wen X, Wei Y, Peng X, Li H, et al. Effect of matrine on HeLa cell adhesion and migration. Eur J Pharmacol. 2007;563(1–3):69–76.
38. Wheeler DL, Iida M, Dunn EF. The Role of Src in Solid Tumors. Oncologist. 2009;14(7):667–78.
39. Levin VA. Basis and importance of Src as a target in cancer. Cancer Treat Res. 2004;119:89–119.
40. Martellucci S, Clementi L, Sabetta S, Mattei V, Botta L, Angelucci A. Src Family Kinases as Therapeutic Targets in Advanced Solid Tumors: What We Have Learned so Far. Cancers (Basel). 2020;12(6):1448.
41. Bowman T, Broome MA, Sinibaldi D, Wharton W, Pledger WJ, Sedivy JM, et al. Stat3-mediated Myc expression is required for Src transformation and PDGF-induced mitogenesis. Proc Natl Acad Sci U S A. 2001;98(13):7319–24.

Figures

Fig.1

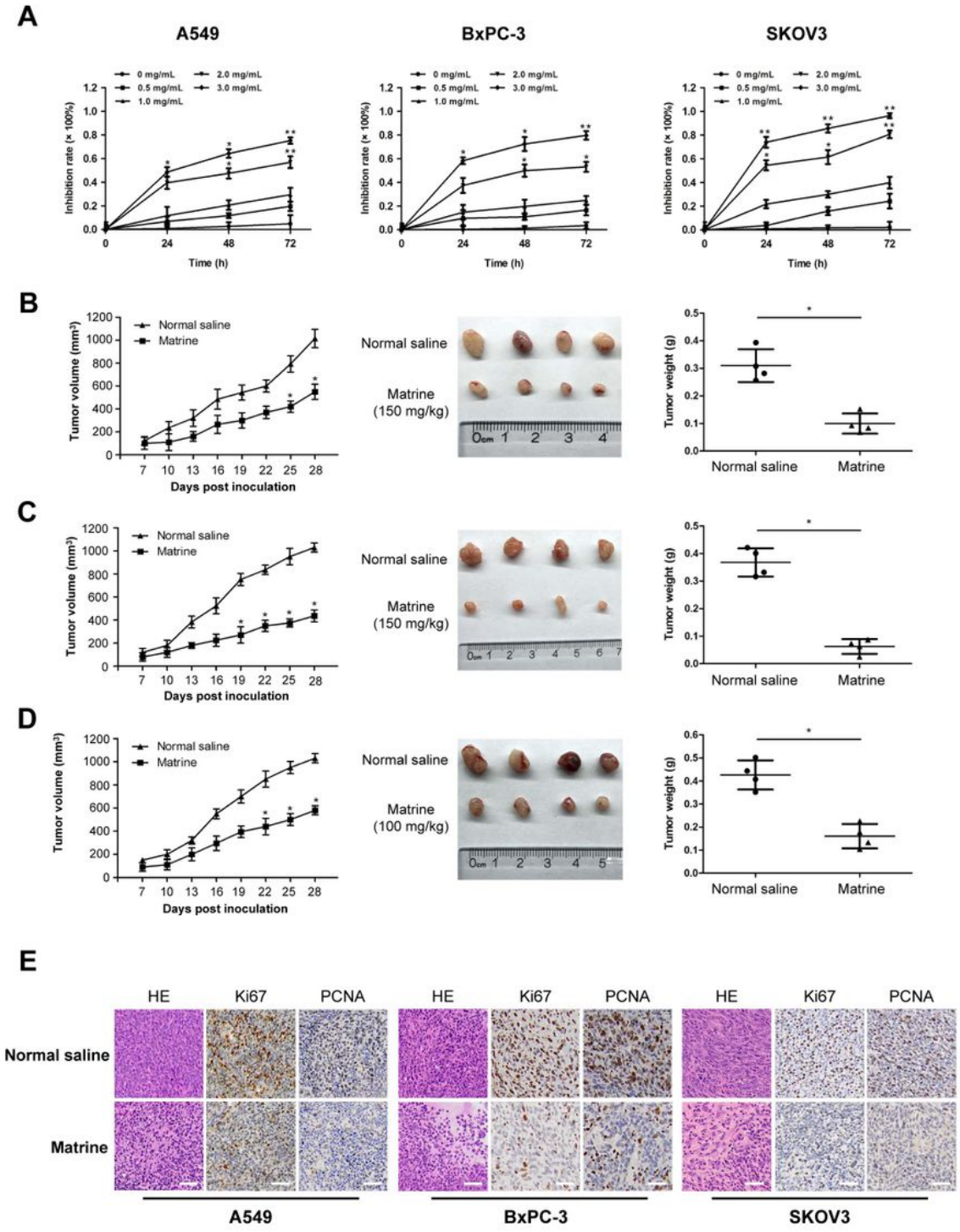

Figure 1

Matrine inhibited the proliferation of cancer cells in vitro and in vivo. a Human non-small cell lung cancer cell A549, human pancreatic cancer cell BxPC-3 and human ovarian cancer cell SKOV3 were treated with matrine at concentrations of 0, 0.5, 1.0, 2.0 and 3.0 mg/mL for 0, 24, 48 and 72 h, respectively. MTT assay was conducted to examine the effect of matrine on the proliferation of cancer cells. Data are presented as mean ± SD (*P < 0.05, **P < 0.01). b-d Xenograft models were established by subcutaneous

injection of A549 (b), BxPC-3 (c) and SKOV3 (d) cells in BALB/c nude mice, respectively. Tumor volume, size and weight in matrine-treated mice were significantly smaller than those in normal saline-treated mice (150 mg/kg in A549 and BxPC-3 cells, 100 mg/kg in SKOV3 cells, ip). Data are presented as mean ± SD (n = 4, *P < 0.05). e The representative histological examinations of dissected tumors of mice inoculated with A549, BxPC-3 and SKOV3 cells after matrine or normal saline treatment. Scale bar: 50 μm.

Fig.1

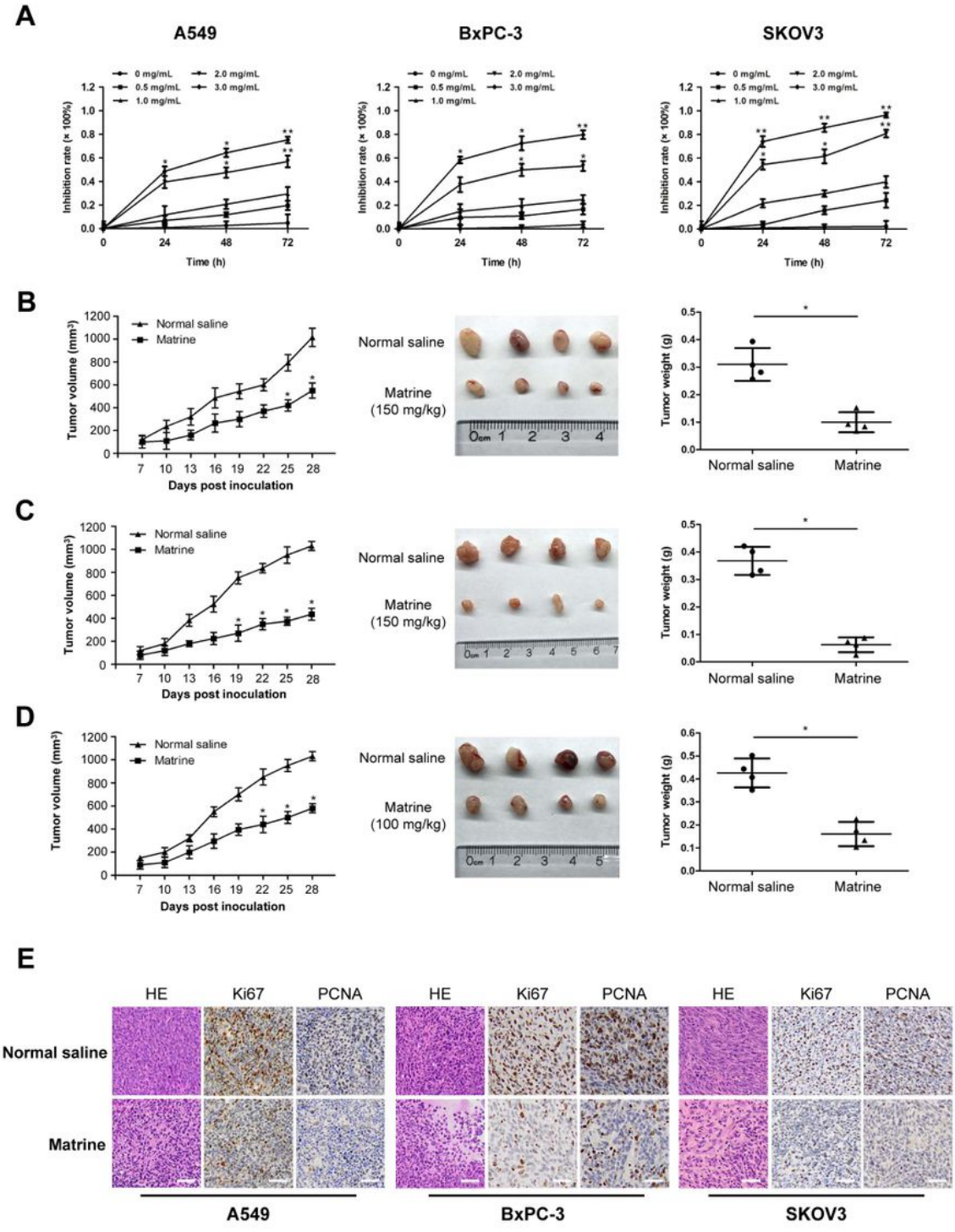

Figure 1

Matrine inhibited the proliferation of cancer cells in vitro and in vivo. a Human non-small cell lung cancer cell A549, human pancreatic cancer cell BxPC-3 and human ovarian cancer cell SKOV3 were treated with matrine at concentrations of 0, 0.5, 1.0, 2.0 and 3.0 mg/mL for 0, 24, 48 and 72 h, respectively. MTT assay was conducted to examine the effect of matrine on the proliferation of cancer cells. Data are presented as mean ± SD (*P < 0.05, **P < 0.01). b-d Xenograft models were established by subcutaneous injection of A549 (b), BxPC-3 (c) and SKOV3 (d) cells in BALB/c nude mice, respectively. Tumor volume, size and weight in matrine-treated mice were significantly smaller than those in normal saline-treated mice (150 mg/kg in A549 and BxPC-3 cells, 100 mg/kg in SKOV3 cells, ip). Data are presented as mean ± SD (n = 4, *P < 0.05). e The representative histological examinations of dissected tumors of mice inoculated with A549, BxPC-3 and SKOV3 cells after matrine or normal saline treatment. Scale bar: 50 μm.

Fig.1

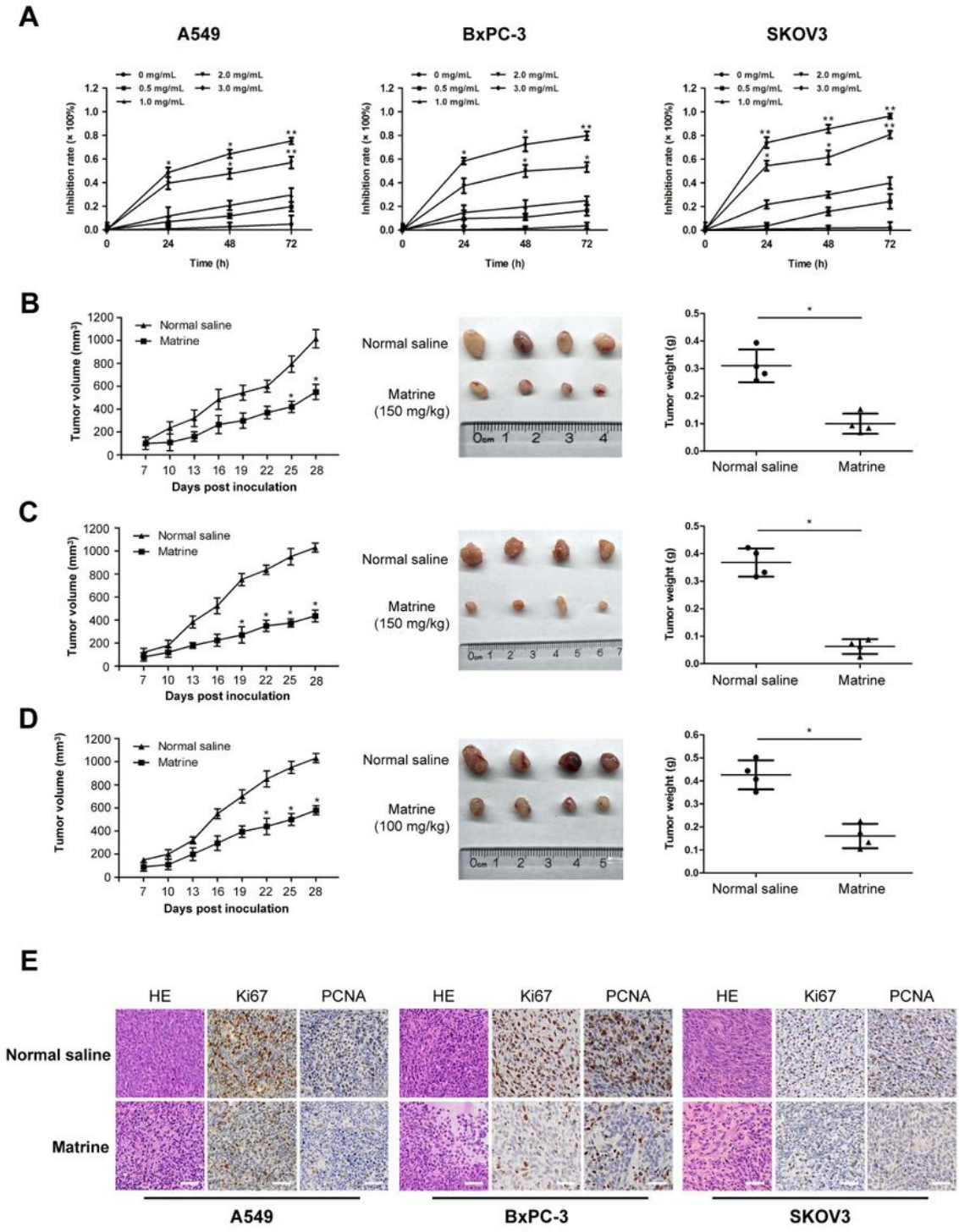

Figure 1

Matrine inhibited the proliferation of cancer cells in vitro and in vivo. a Human non-small cell lung cancer cell A549, human pancreatic cancer cell BxPC-3 and human ovarian cancer cell SKOV3 were treated with matrine at concentrations of 0, 0.5, 1.0, 2.0 and 3.0 mg/mL for 0, 24, 48 and 72 h, respectively. MTT assay was conducted to examine the effect of matrine on the proliferation of cancer cells. Data are presented as mean ± SD (*P < 0.05, **P < 0.01). b-d Xenograft models were established by subcutaneous

injection of A549 (b), BxPC-3 (c) and SKOV3 (d) cells in BALB/c nude mice, respectively. Tumor volume, size and weight in matrine-treated mice were significantly smaller than those in normal saline-treated mice (150 mg/kg in A549 and BxPC-3 cells, 100 mg/kg in SKOV3 cells, ip). Data are presented as mean ± SD (n = 4, *P < 0.05). e The representative histological examinations of dissected tumors of mice inoculated with A549, BxPC-3 and SKOV3 cells after matrine or normal saline treatment. Scale bar: 50 μm.

Fig.2

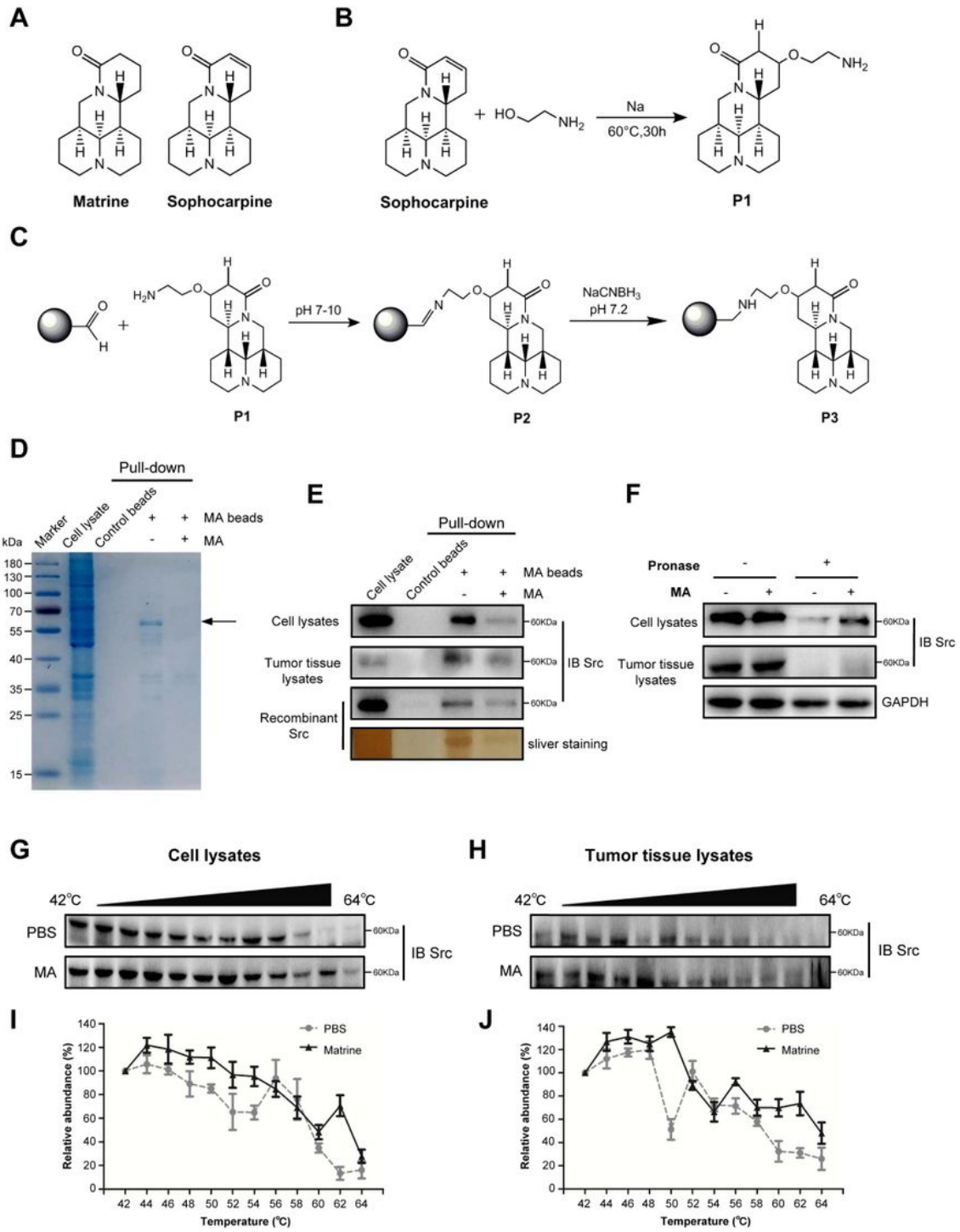

Figure 2

Matrine targeted Src protein. a Chemical structure of matrine and sophocarpine. b The synthesis scheme of 13α-(2-amino) ethoxymatrine (P1). c Synthesis of matrine-amino coupling resins (MA beads, P3). d SKOV3 cell lysates were incubated with control beads, MA beads and MA beads in the presence of matrine (2.0 mg/mL). Protein affinity pull-down assay was performed and the matrine-bound proteins were separated by SDS-PAGE. The gels were processed by Coomassie brilliant blue staining. e Pull-down assays were performed using cell lysates, tumor tissue lysates and recombinant protein GST-Src. The cell lysates, tumor tissue lysates and recombinant proteins were incubated with control beads, MA beads or MA beads in the presence of matrine (2.0 mg/mL). The mixtures were blotted for Src and sliver staining. f DARTS results for pronase-digested cell lysates and tumor tissues. Cell lysates and tumor tissue lysates were prepared with matrine or PBS for 1 h, followed by digestion with pronase. Western blotting showed protection of the target protein Src, whereas digestion of the non-target proteins GAPDH is unchanged by matrine. g, h CETSA was performed in cell lysates (g) and tumor tissue lysates (h) treated with matrine or PBS. The stabilization of matrine on Src protein was evaluated by immunoblot. i, j CETSA curves in cell lysates (i) and tumor tissue lysates (j) treated with matrine or PBS. Data are presented as mean ± SD, n = 3 independent experiments.

Fig.2

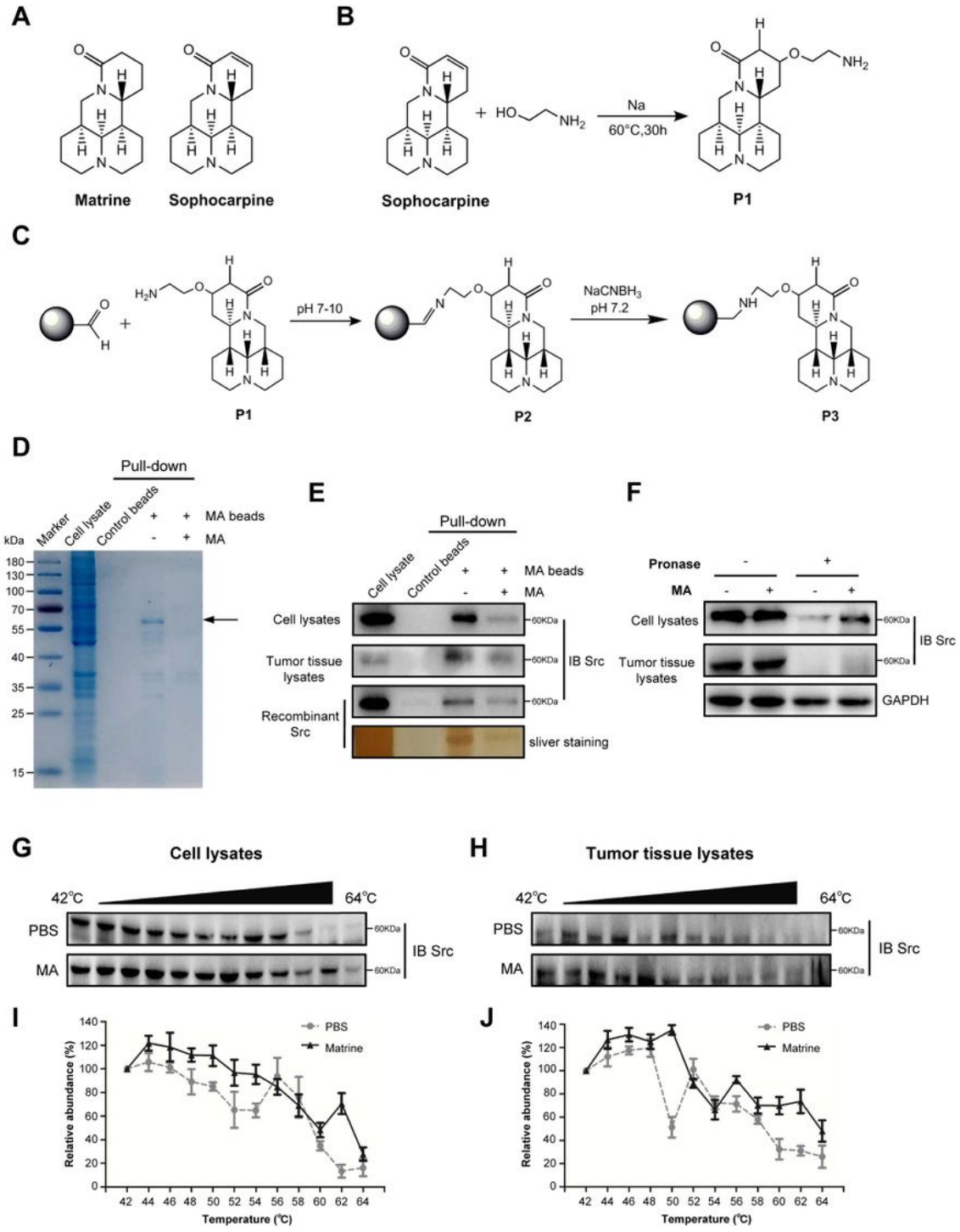

Figure 2

Matrine targeted Src protein. a Chemical structure of matrine and sophocarpine. b The synthesis scheme of 13α-(2-amino) ethoxymatrine (P1). c Synthesis of matrine-amino coupling resins (MA beads, P3). d SKOV3 cell lysates were incubated with control beads, MA beads and MA beads in the presence of matrine (2.0 mg/mL). Protein affinity pull-down assay was performed and the matrine-bound proteins were separated by SDS-PAGE. The gels were processed by Coomassie brilliant blue staining. e Pull-down

assays were performed using cell lysates, tumor tissue lysates and recombinant protein GST-Src. The cell lysates, tumor tissue lysates and recombinant proteins were incubated with control beads, MA beads or MA beads in the presence of matrine (2.0 mg/mL). The mixtures were blotted for Src and sliver staining. f DARTS results for pronase-digested cell lysates and tumor tissues. Cell lysates and tumor tissue lysates were prepared with matrine or PBS for 1 h, followed by digestion with pronase. Western blotting showed protection of the target protein Src, whereas digestion of the non-target proteins GAPDH is unchanged by matrine. g, h CETSA was performed in cell lysates (g) and tumor tissue lysates (h) treated with matrine or PBS. The stabilization of matrine on Src protein was evaluated by immunoblot. i, j CETSA curves in cell lysates (i) and tumor tissue lysates (j) treated with matrine or PBS. Data are presented as mean ± SD, n = 3 independent experiments.

Fig.2

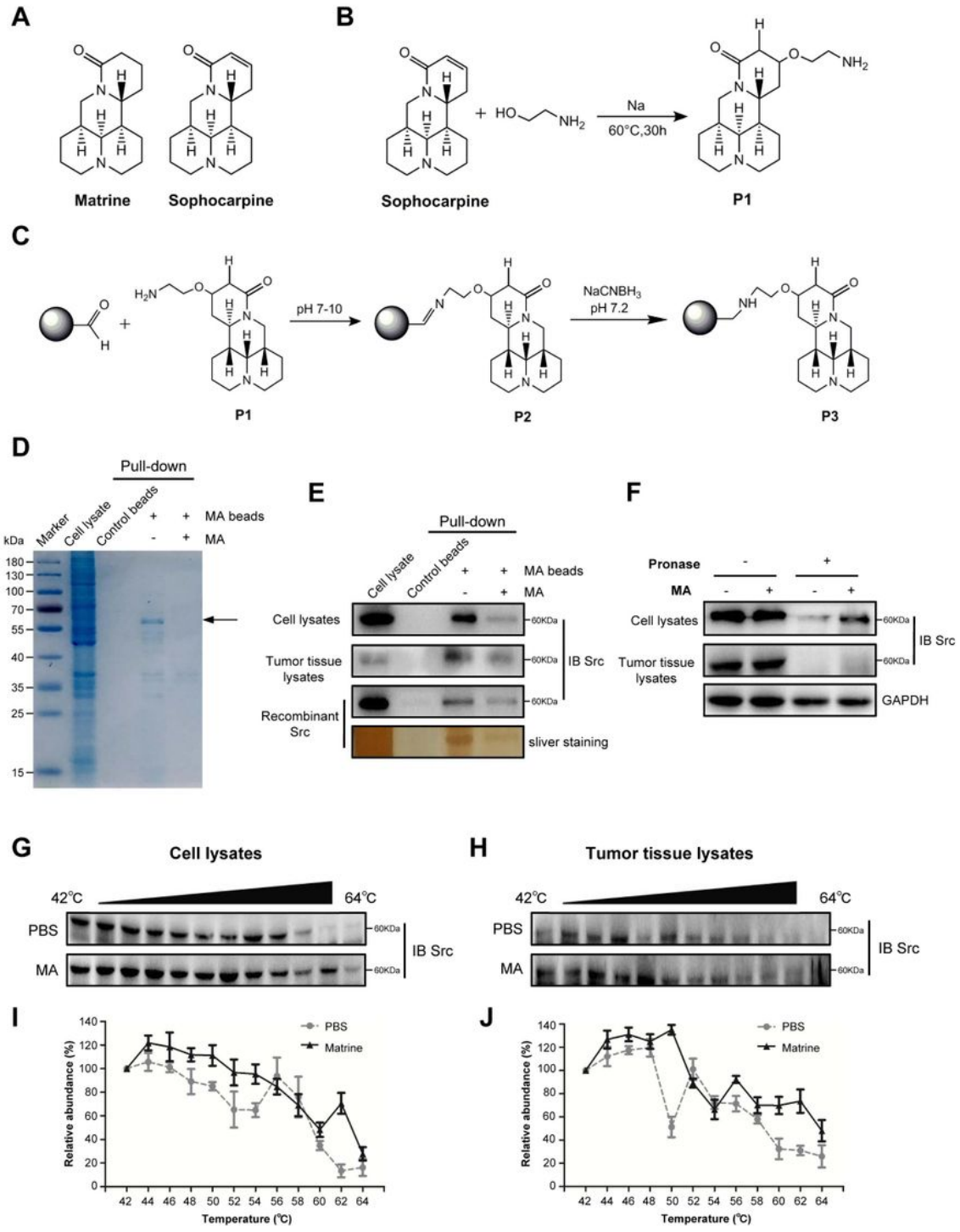

Figure 2

Matrine targeted Src protein. a Chemical structure of matrine and sophocarpine. b The synthesis scheme of 13α-(2-amino) ethoxymatrine (P1). c Synthesis of matrine-amino coupling resins (MA beads, P3). d SKOV3 cell lysates were incubated with control beads, MA beads and MA beads in the presence of matrine (2.0 mg/mL). Protein affinity pull-down assay was performed and the matrine-bound proteins were separated by SDS-PAGE. The gels were processed by Coomassie brilliant blue staining. e Pull-down

assays were performed using cell lysates, tumor tissue lysates and recombinant protein GST-Src. The cell lysates, tumor tissue lysates and recombinant proteins were incubated with control beads, MA beads or MA beads in the presence of matrine (2.0 mg/mL). The mixtures were blotted for Src and sliver staining. f DARTS results for pronase-digested cell lysates and tumor tissues. Cell lysates and tumor tissue lysates were prepared with matrine or PBS for 1 h, followed by digestion with pronase. Western blotting showed protection of the target protein Src, whereas digestion of the non-target proteins GAPDH is unchanged by matrine. g, h CETSA was performed in cell lysates (g) and tumor tissue lysates (h) treated with matrine or PBS. The stabilization of matrine on Src protein was evaluated by immunoblot. i, j CETSA curves in cell lysates (i) and tumor tissue lysates (j) treated with matrine or PBS. Data are presented as mean ± SD, n = 3 independent experiments.

Fig.3

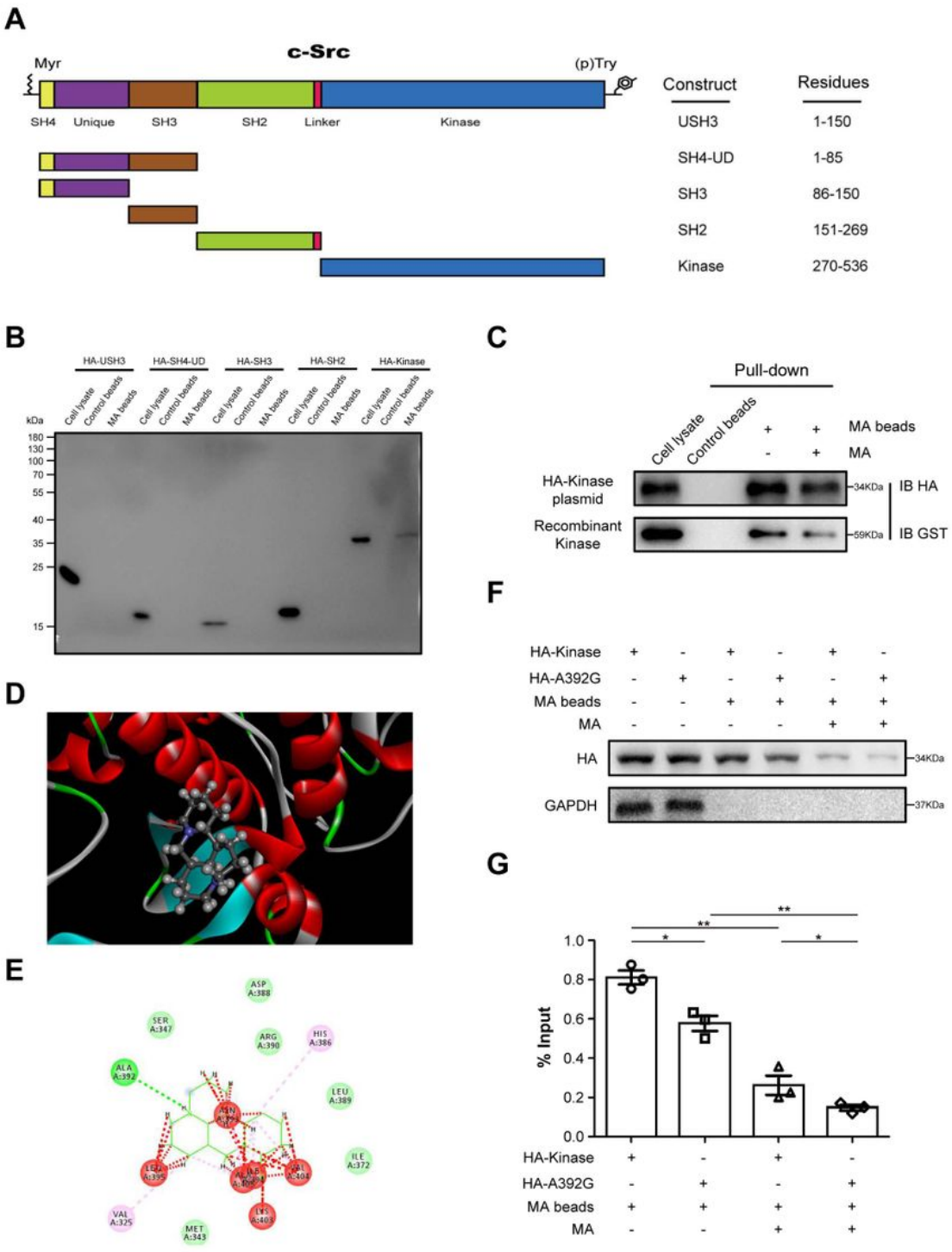

Figure 3

Src kinase domain was required for its interaction with matrine. a Schematic of constructs with different functional domains of Src. USH3: 1-150 aa, SH4-UD: 1-85 aa, SH3: 86-150 aa, SH2: 151-269 aa, Kinase: 270-536 aa. b HA-tagged deletion constructs of Src, including HA-USH3, HA-SH4-UD, HA-SH3, HA-SH2 and HA-Kinase, were transfected into HEK-293 cells, respectively. Cell lysates were harvested and incubated with MA beads or control beads and blotted by anti-HA. c Constructs containing Src kinase domain were

overexpressed in HEK-293 cells and expressed in BL21 cells, respectively. Competition assay results showed that cell lysates transfected with HA-Kinase plasmid and recombinant protein were pulled down by MA beads, which were reduced by adding an excess amount of MA. d Molecular docking diagram of matrine bound to Src kinase domain (PDB: 1YOJ). Matrine depicted as the ball-and-stick model showing carbon (gray), hydrogen (white), oxygen (red) and nitrogen (blue) atoms. e Hydrogen bonds between matrine and Src kinase domain were identified and indicated by green line. Van der Waals forces between matrine and Src kinase domain were indicated by pale green circles. f HEK-293 cells were transfected with plasmids pcDNA3.1-HA-Kinase and pcDNA3.1-HA-Kinase-A392G, respectively. MA beads were added to cell lysates for pull-down assay to detect matrine binding. g Densitometric quantification data of matrine binding followed by pull-down assay. Data are presented as mean ± SD (n = 3, *P < 0.05, **P < 0.01).

Fig.3

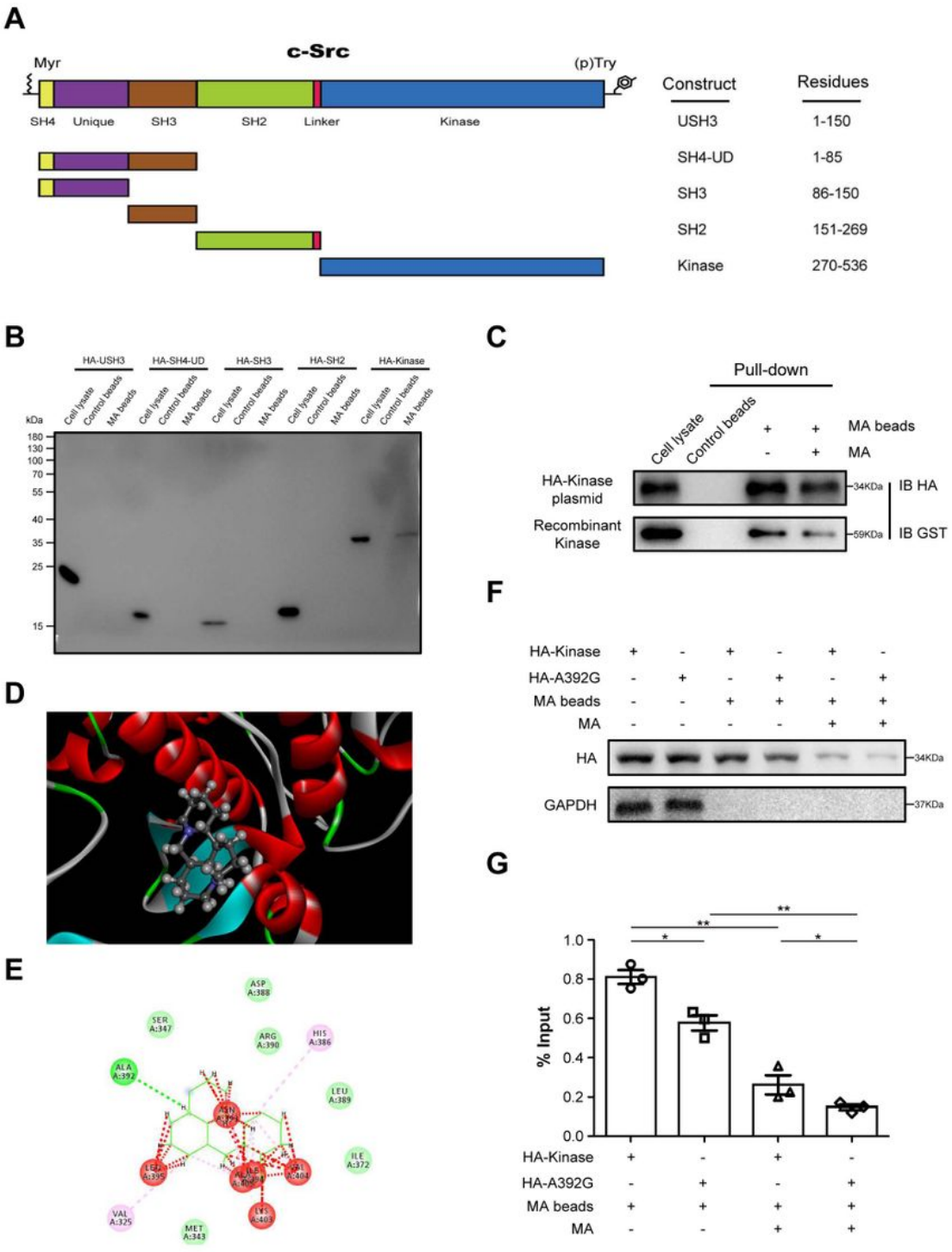

Figure 3

Src kinase domain was required for its interaction with matrine. a Schematic of constructs with different functional domains of Src. USH3: 1-150 aa, SH4-UD: 1-85 aa, SH3: 86-150 aa, SH2: 151-269 aa, Kinase: 270-536 aa. b HA-tagged deletion constructs of Src, including HA-USH3, HA-SH4-UD, HA-SH3, HA-SH2 and HA-Kinase, were transfected into HEK-293 cells, respectively. Cell lysates were harvested and incubated with MA beads or control beads and blotted by anti-HA. c Constructs containing Src kinase domain were

overexpressed in HEK-293 cells and expressed in BL21 cells, respectively. Competition assay results showed that cell lysates transfected with HA-Kinase plasmid and recombinant protein were pulled down by MA beads, which were reduced by adding an excess amount of MA. d Molecular docking diagram of matrine bound to Src kinase domain (PDB: 1YOJ). Matrine depicted as the ball-and-stick model showing carbon (gray), hydrogen (white), oxygen (red) and nitrogen (blue) atoms. e Hydrogen bonds between matrine and Src kinase domain were identified and indicated by green line. Van der Waals forces between matrine and Src kinase domain were indicated by pale green circles. f HEK-293 cells were transfected with plasmids pcDNA3.1-HA-Kinase and pcDNA3.1-HA-Kinase-A392G, respectively. MA beads were added to cell lysates for pull-down assay to detect matrine binding. g Densitometric quantification data of matrine binding followed by pull-down assay. Data are presented as mean ± SD (n = 3, *P < 0.05, **P < 0.01).

Fig.3

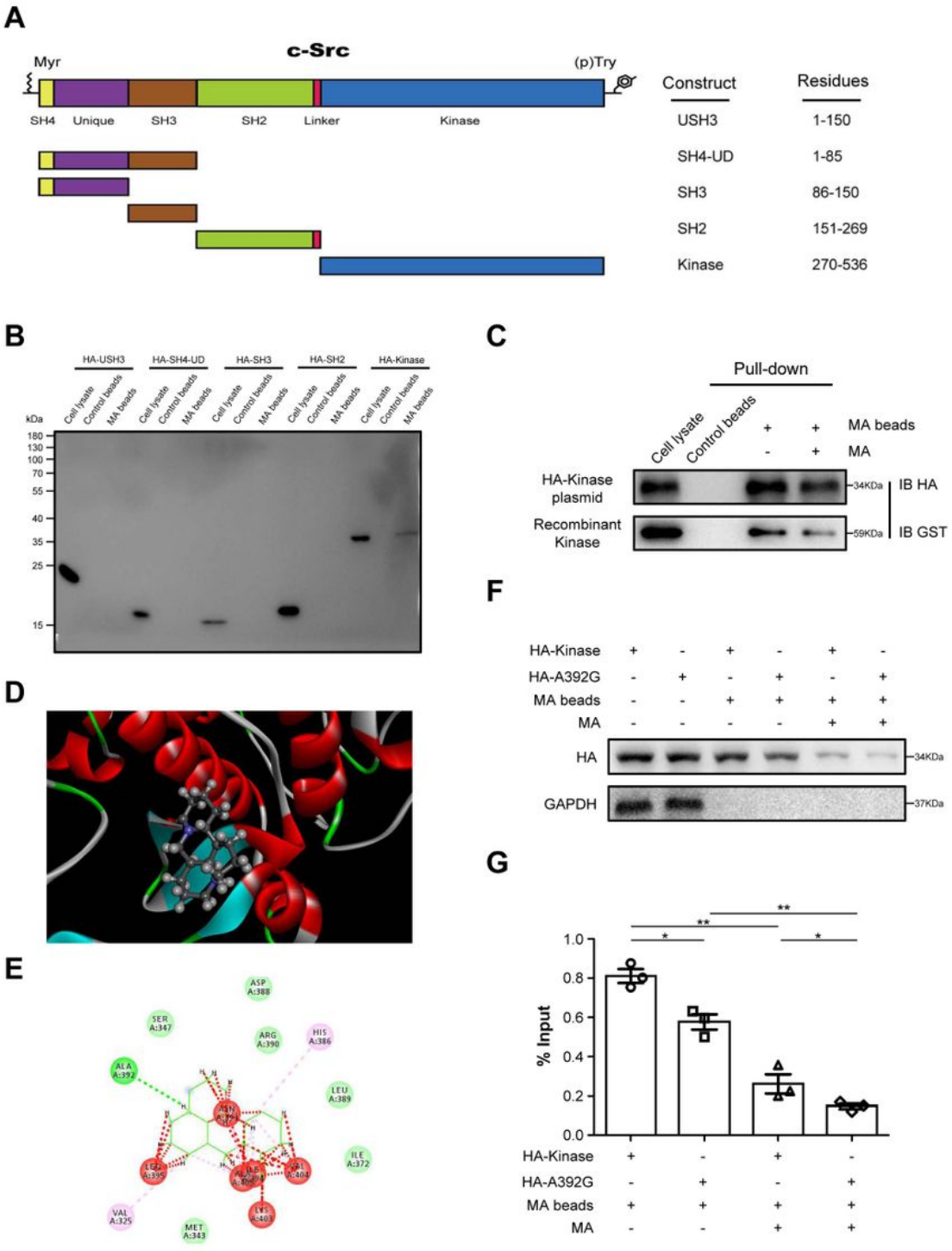

Figure 3

Src kinase domain was required for its interaction with matrine. a Schematic of constructs with different functional domains of Src. USH3: 1-150 aa, SH4-UD: 1-85 aa, SH3: 86-150 aa, SH2: 151-269 aa, Kinase: 270-536 aa. b HA-tagged deletion constructs of Src, including HA-USH3, HA-SH4-UD, HA-SH3, HA-SH2 and HA-Kinase, were transfected into HEK-293 cells, respectively. Cell lysates were harvested and incubated with MA beads or control beads and blotted by anti-HA. c Constructs containing Src kinase domain were

overexpressed in HEK-293 cells and expressed in BL21 cells, respectively. Competition assay results showed that cell lysates transfected with HA-Kinase plasmid and recombinant protein were pulled down by MA beads, which were reduced by adding an excess amount of MA. d Molecular docking diagram of matrine bound to Src kinase domain (PDB: 1YOJ). Matrine depicted as the ball-and-stick model showing carbon (gray), hydrogen (white), oxygen (red) and nitrogen (blue) atoms. e Hydrogen bonds between matrine and Src kinase domain were identified and indicated by green line. Van der Waals forces between matrine and Src kinase domain were indicated by pale green circles. f HEK-293 cells were transfected with plasmids pcDNA3.1-HA-Kinase and pcDNA3.1-HA-Kinase-A392G, respectively. MA beads were added to cell lysates for pull-down assay to detect matrine binding. g Densitometric quantification data of matrine binding followed by pull-down assay. Data are presented as mean ± SD (n = 3, *P < 0.05, **P < 0.01).

Fig.4

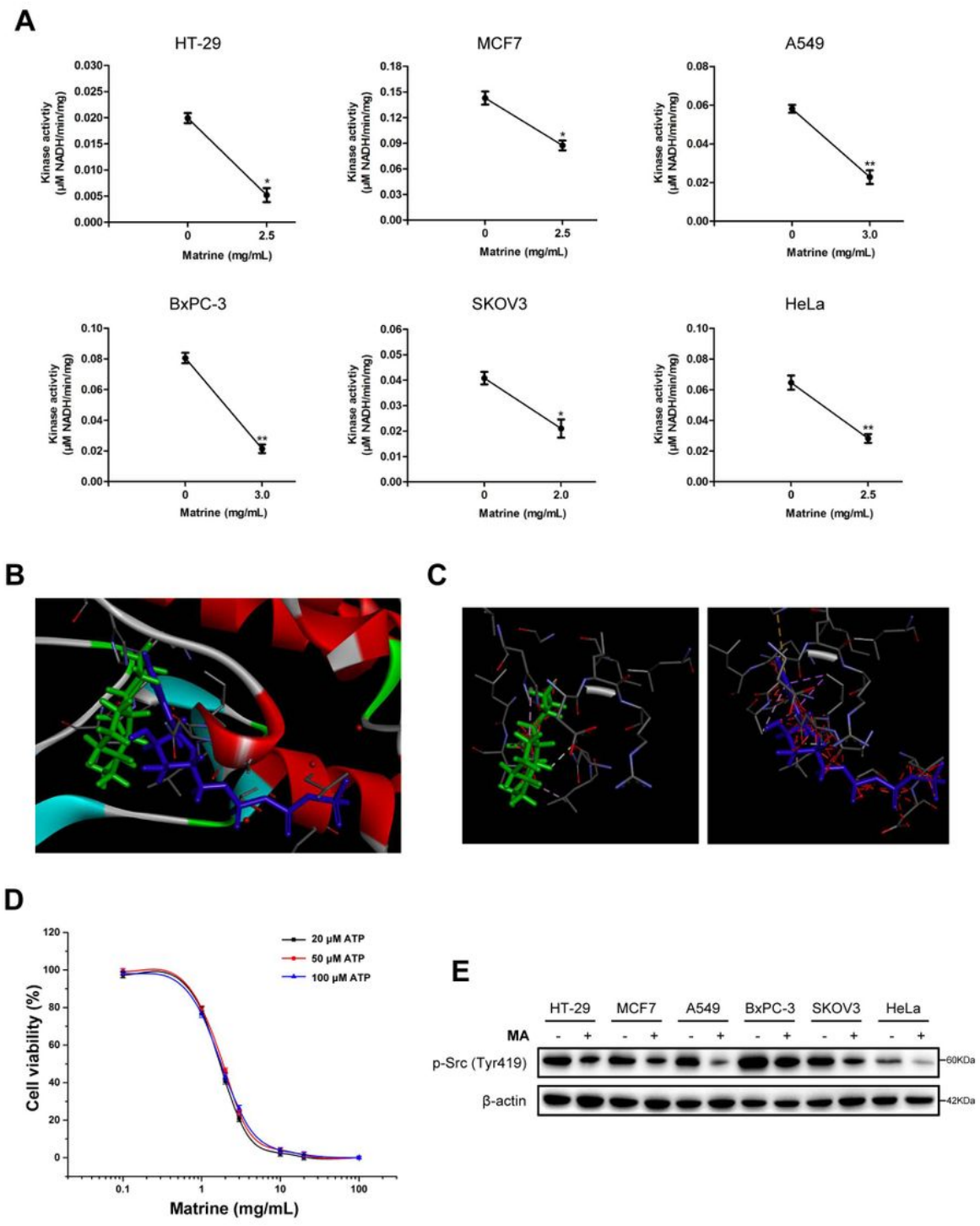

Figure 4

Matrine was a non-ATP-competitive inhibitor of Src kinase. a The effect of matrine on Src kinase activity in cancer cells, including HT-29, MCF7, A549, BxPC-3, SKOV3 and HeLa, were determined according to the instructions of Src kinase activity detection kit (*P < 0.05, **P < 0.01). b,c Schematic diagram of matrine and ATP bound to Src kinase domain. Matrine (green) and ATP (bule) molecules were depicted as the ball-and-stick models. d Dose-response curves of matrine against Src kinase at various ATP

concentrations. Data are the mean ± SD of three independent experiments. e HT-29, MCF7, A549, BxPC-3, SKOV3 and HeLa cells were exposed to matrine at its optimal concentrations for 24 h, respectively. The effects of matrine on the p-Src (Tyr419) were analyzed by Western blot, respectively. β-actin was used as control.

Fig.4

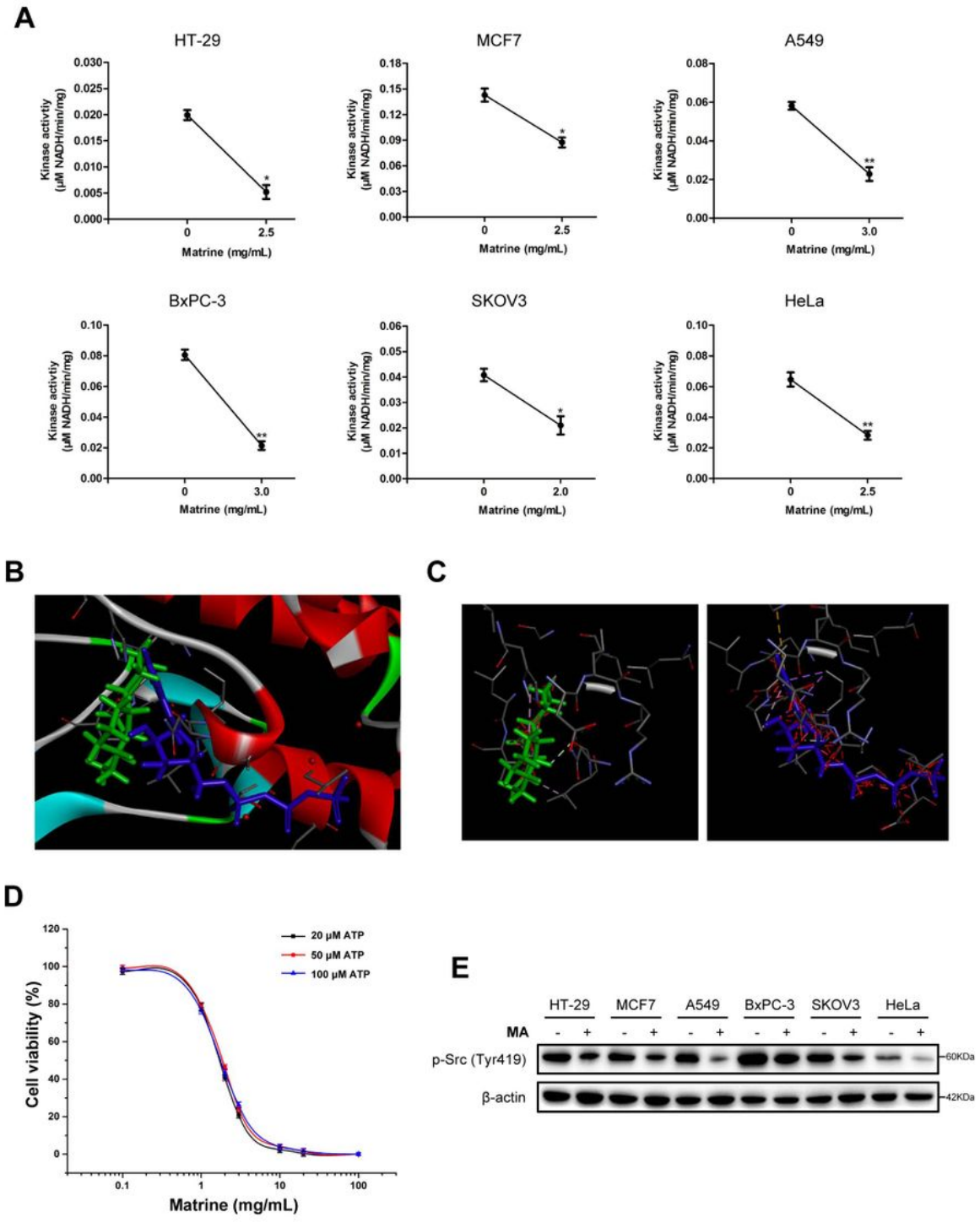

Figure 4

Matrine was a non-ATP-competitive inhibitor of Src kinase. a The effect of matrine on Src kinase activity in cancer cells, including HT-29, MCF7, A549, BxPC-3, SKOV3 and HeLa, were determined according to the instructions of Src kinase activity detection kit (*P < 0.05, **P < 0.01). b,c Schematic diagram of matrine and ATP bound to Src kinase domain. Matrine (green) and ATP (bule) molecules were depicted as the ball-and-stick models. d Dose-response curves of matrine against Src kinase at various ATP concentrations. Data are the mean ± SD of three independent experiments. e HT-29, MCF7, A549, BxPC-3, SKOV3 and HeLa cells were exposed to matrine at its optimal concentrations for 24 h, respectively. The effects of matrine on the p-Src (Tyr419) were analyzed by Western blot, respectively. β-actin was used as control.

Fig.4

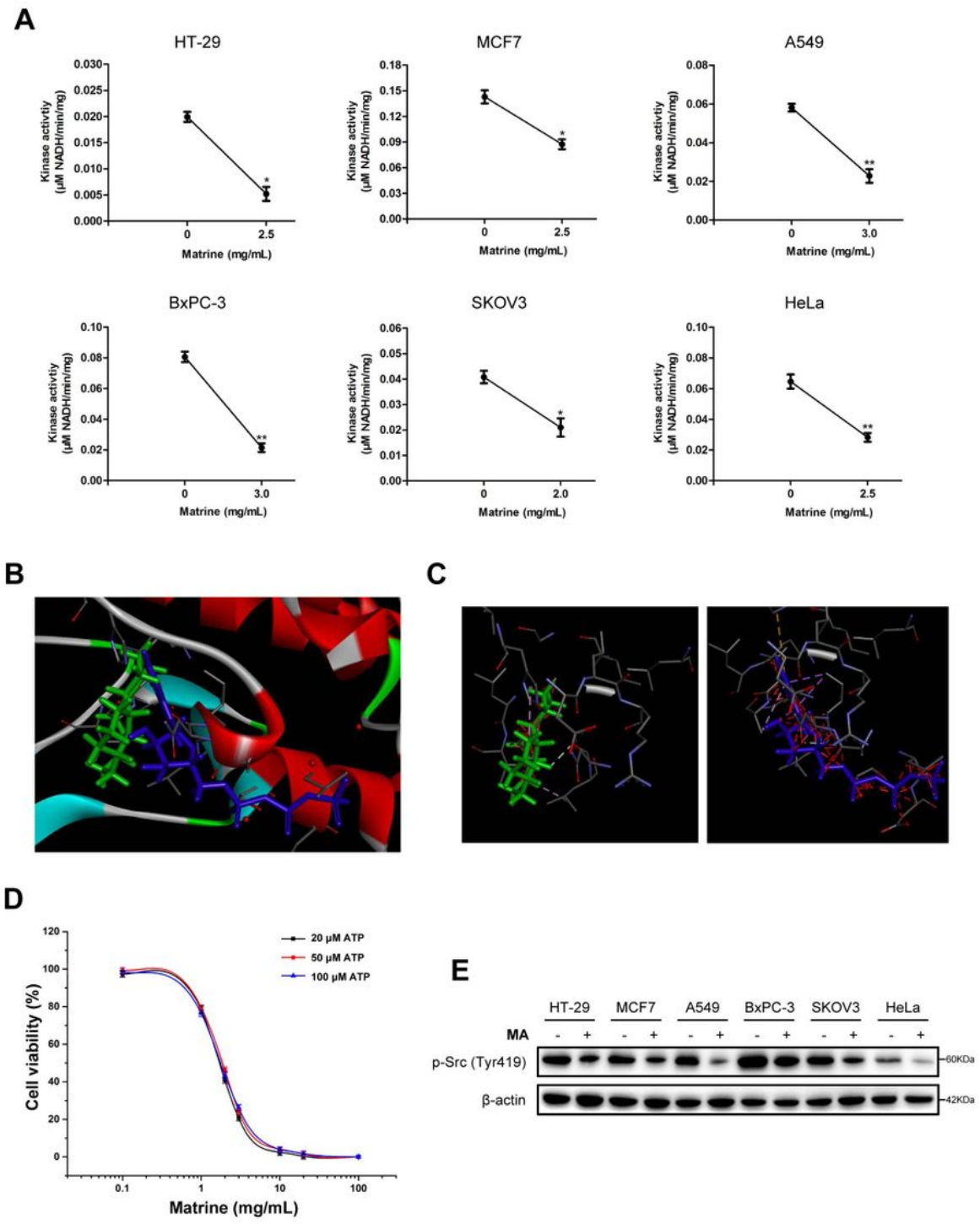

Figure 4

Matrine was a non-ATP-competitive inhibitor of Src kinase. a The effect of matrine on Src kinase activity in cancer cells, including HT-29, MCF7, A549, BxPC-3, SKOV3 and HeLa, were determined according to the instructions of Src kinase activity detection kit (*P < 0.05, **P < 0.01). b,c Schematic diagram of matrine and ATP bound to Src kinase domain. Matrine (green) and ATP (bule) molecules were depicted as the ball-and-stick models. d Dose-response curves of matrine against Src kinase at various ATP

concentrations. Data are the mean ± SD of three independent experiments. e HT-29, MCF7, A549, BxPC-3, SKOV3 and HeLa cells were exposed to matrine at its optimal concentrations for 24 h, respectively. The effects of matrine on the p-Src (Tyr419) were analyzed by Western blot, respectively. β-actin was used as control.

Fig.5

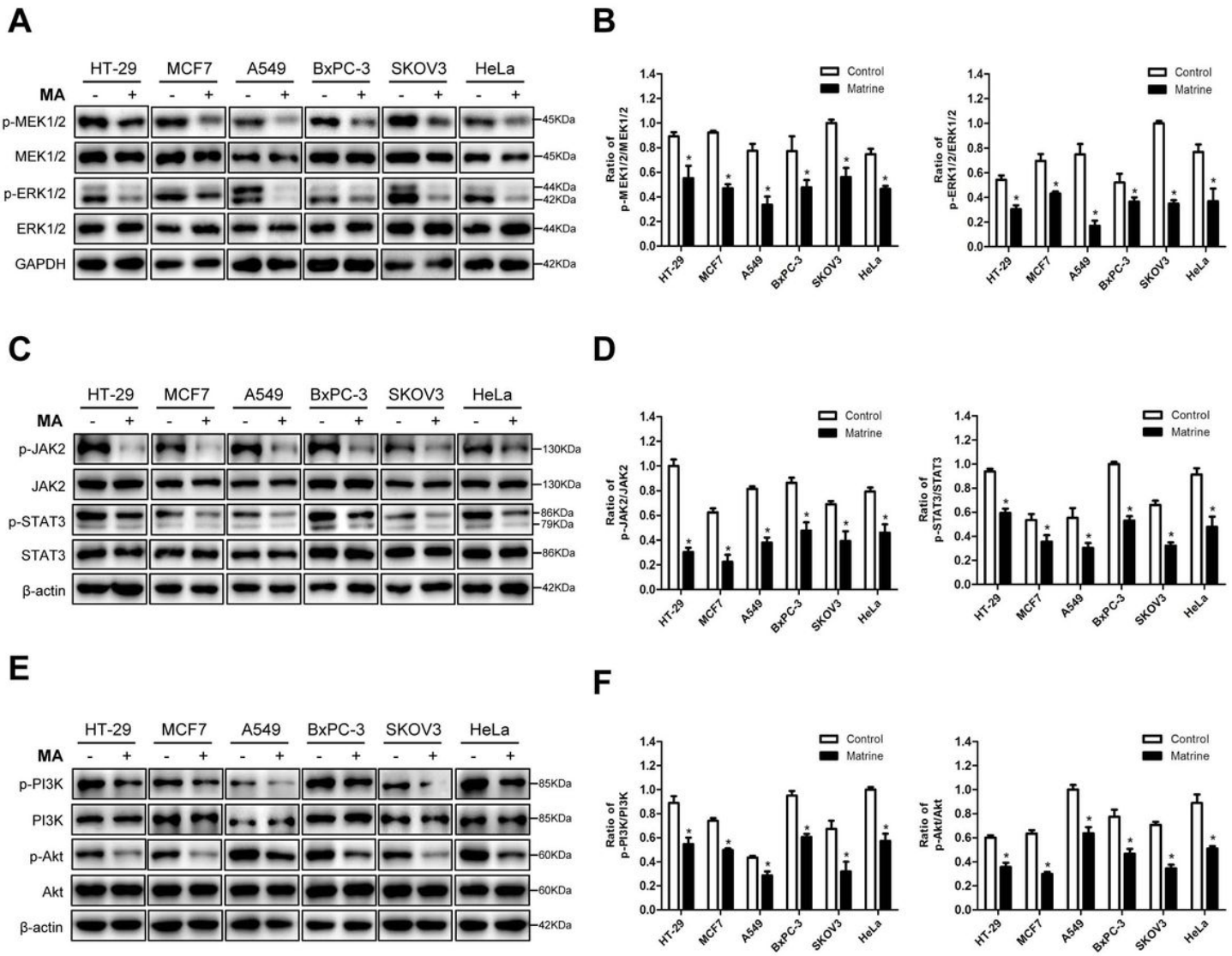

Figure 5

The phosphorylation signaling pathways were inhibited by matrine. a Cancer cells, including HT-29, MCF7, A549, BxPC-3, SKOV3 and HeLa, were treated with matrine at the optimal concentration for 24 h, respectively. The effects of matrine on the phosphorylation levels of MEK1/2 and ERK1/2 in cancer cells were detected by Western blot. GAPDH was used as a loading control. b Histograms indicating the phosphorylation ratio of MEK1/2 and ERK1/2 in cancer cells. Data are presented as mean ± SD (n = 3, *P < 0.05). c Immunoblot analysis showed that the phosphorylation levels of JAK2 and STAT3 in cancer cells were down-regulated by matrine. d The ratio of p-JAK2/JAK2 and p-STAT3/STAT3 were obviously

reduced in cancer cells. Data are presented as mean ± SD (n = 3, *P < 0.05). e After matrine treatment, the phosphorylation levels of PI3K and Akt were markedly decreased in cancer cells. f The bar graphs showed mean ± SD of the phosphorylation ratio of PI3K and Akt in cancer cells from three independent experiments (*P < 0.05).

Fig.5

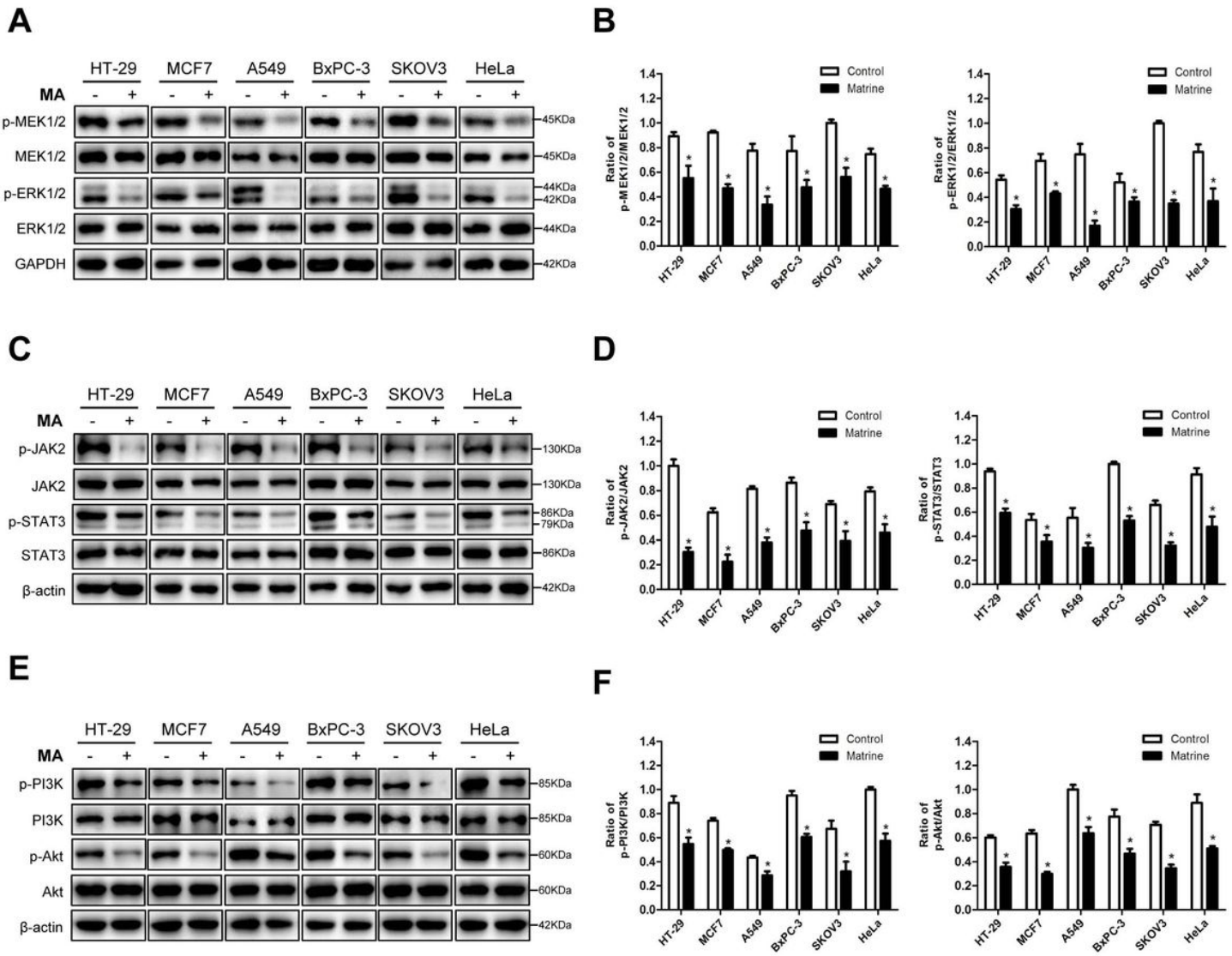

Figure 5

The phosphorylation signaling pathways were inhibited by matrine. a Cancer cells, including HT-29, MCF7, A549, BxPC-3, SKOV3 and HeLa, were treated with matrine at the optimal concentration for 24 h, respectively. The effects of matrine on the phosphorylation levels of MEK1/2 and ERK1/2 in cancer cells were detected by Western blot. GAPDH was used as a loading control. b Histograms indicating the phosphorylation ratio of MEK1/2 and ERK1/2 in cancer cells. Data are presented as mean ± SD (n = 3, *P < 0.05). c Immunoblot analysis showed that the phosphorylation levels of JAK2 and STAT3 in cancer cells were down-regulated by matrine. d The ratio of p-JAK2/JAK2 and p-STAT3/STAT3 were obviously

reduced in cancer cells. Data are presented as mean ± SD (n = 3, *P < 0.05). e After matrine treatment, the phosphorylation levels of PI3K and Akt were markedly decreased in cancer cells. f The bar graphs showed mean ± SD of the phosphorylation ratio of PI3K and Akt in cancer cells from three independent experiments (*P < 0.05).

Fig.5

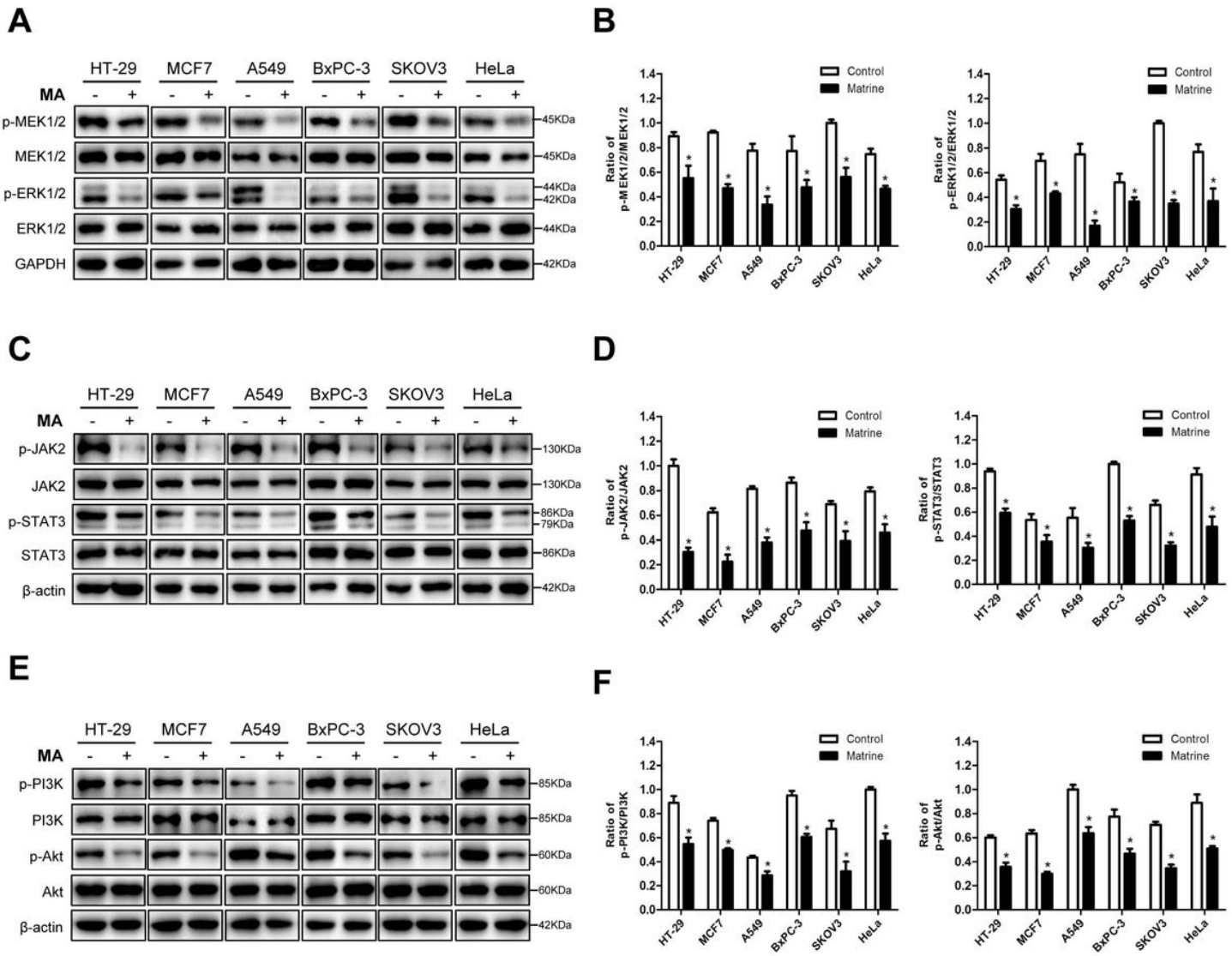

Figure 5

The phosphorylation signaling pathways were inhibited by matrine. a Cancer cells, including HT-29, MCF7, A549, BxPC-3, SKOV3 and HeLa, were treated with matrine at the optimal concentration for 24 h, respectively. The effects of matrine on the phosphorylation levels of MEK1/2 and ERK1/2 in cancer cells were detected by Western blot. GAPDH was used as a loading control. b Histograms indicating the phosphorylation ratio of MEK1/2 and ERK1/2 in cancer cells. Data are presented as mean ± SD (n = 3, *P < 0.05). c Immunoblot analysis showed that the phosphorylation levels of JAK2 and STAT3 in cancer cells were down-regulated by matrine. d The ratio of p-JAK2/JAK2 and p-STAT3/STAT3 were obviously

reduced in cancer cells. Data are presented as mean ± SD (n = 3, *P < 0.05). e After matrine treatment, the phosphorylation levels of PI3K and Akt were markedly decreased in cancer cells. f The bar graphs showed mean ± SD of the phosphorylation ratio of PI3K and Akt in cancer cells from three independent experiments (*P < 0.05).

Fig.6

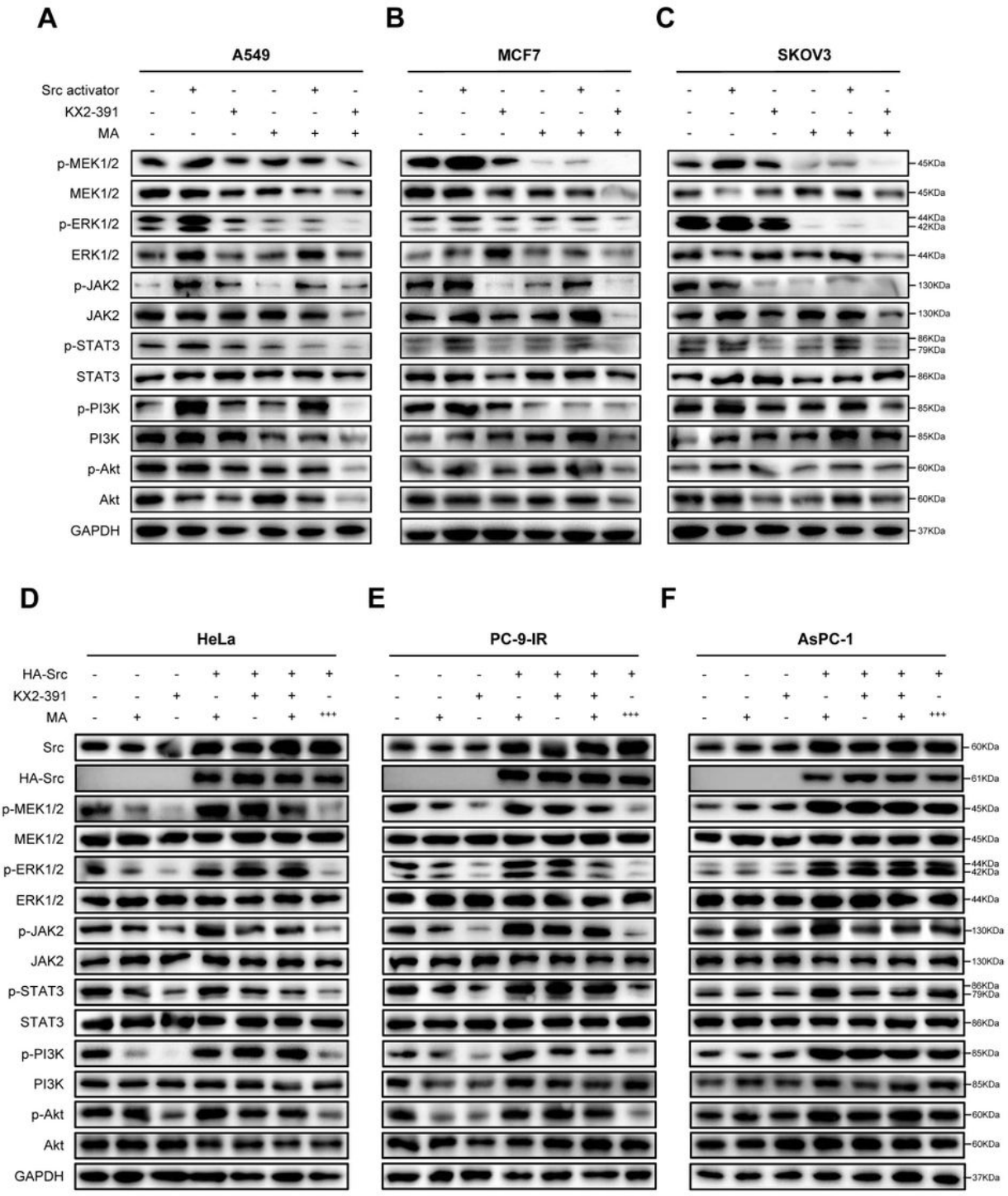

Figure 6

Involvement of Src in matrine-mediated phosphorylation signaling pathways. a-c A549, MCF7 and SKOV3 cells were treated with Src activator or Src inhibitor KX2-391, then exposed to matrine at its optimal concentrations for 24 h, respectively. The phosphorylation levels of MAPK/ERK, JAK2/STAT3 and PI3K/Akt signaling pathways in A549 (a), MCF7 (b) and SKOV3 (c) cells were examined, respectively. d-f Human cervical cancer cell HeLa, gefitinib-resistant human lung cancer cell PC-9-IR and human pancreatic cancer cell AsPC-1 were transfected with plasmid pcDNA3.1-HA-Src, then treated with matrine, KX2-391 and excessive matrine, respectively. The phosphorylation levels of MEK1/2, ERK1/2, JAK2, STAT3, PI3K and Akt in HeLa (d), PC-9-IR (e) and AsPC-1 (f) were detected by Western blot, respectively. GAPDH was used as control.

Fig.6

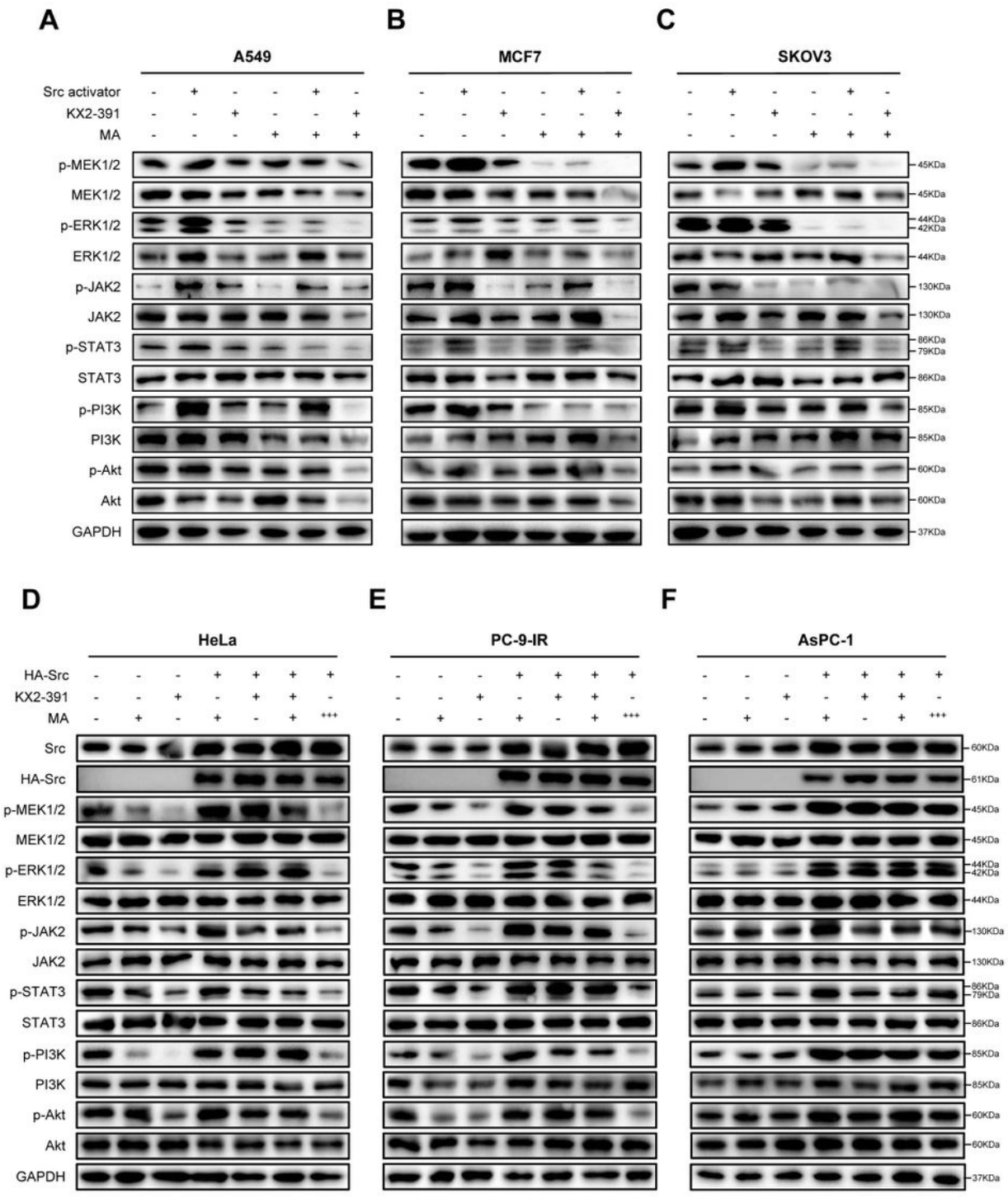

Figure 6

Involvement of Src in matrine-mediated phosphorylation signaling pathways. a-c A549, MCF7 and SKOV3 cells were treated with Src activator or Src inhibitor KX2-391, then exposed to matrine at its optimal concentrations for 24 h, respectively. The phosphorylation levels of MAPK/ERK, JAK2/STAT3 and PI3K/Akt signaling pathways in A549 (a), MCF7 (b) and SKOV3 (c) cells were examined, respectively. d-f Human cervical cancer cell HeLa, gefitinib-resistant human lung cancer cell PC-9-IR and human

pancreatic cancer cell AsPC-1 were transfected with plasmid pcDNA3.1-HA-Src, then treated with matrine, KX2-391 and excessive matrine, respectively. The phosphorylation levels of MEK1/2, ERK1/2, JAK2, STAT3, PI3K and Akt in HeLa (d), PC-9-IR (e) and AsPC-1 (f) were detected by Western blot, respectively. GAPDH was used as control.

Fig.6

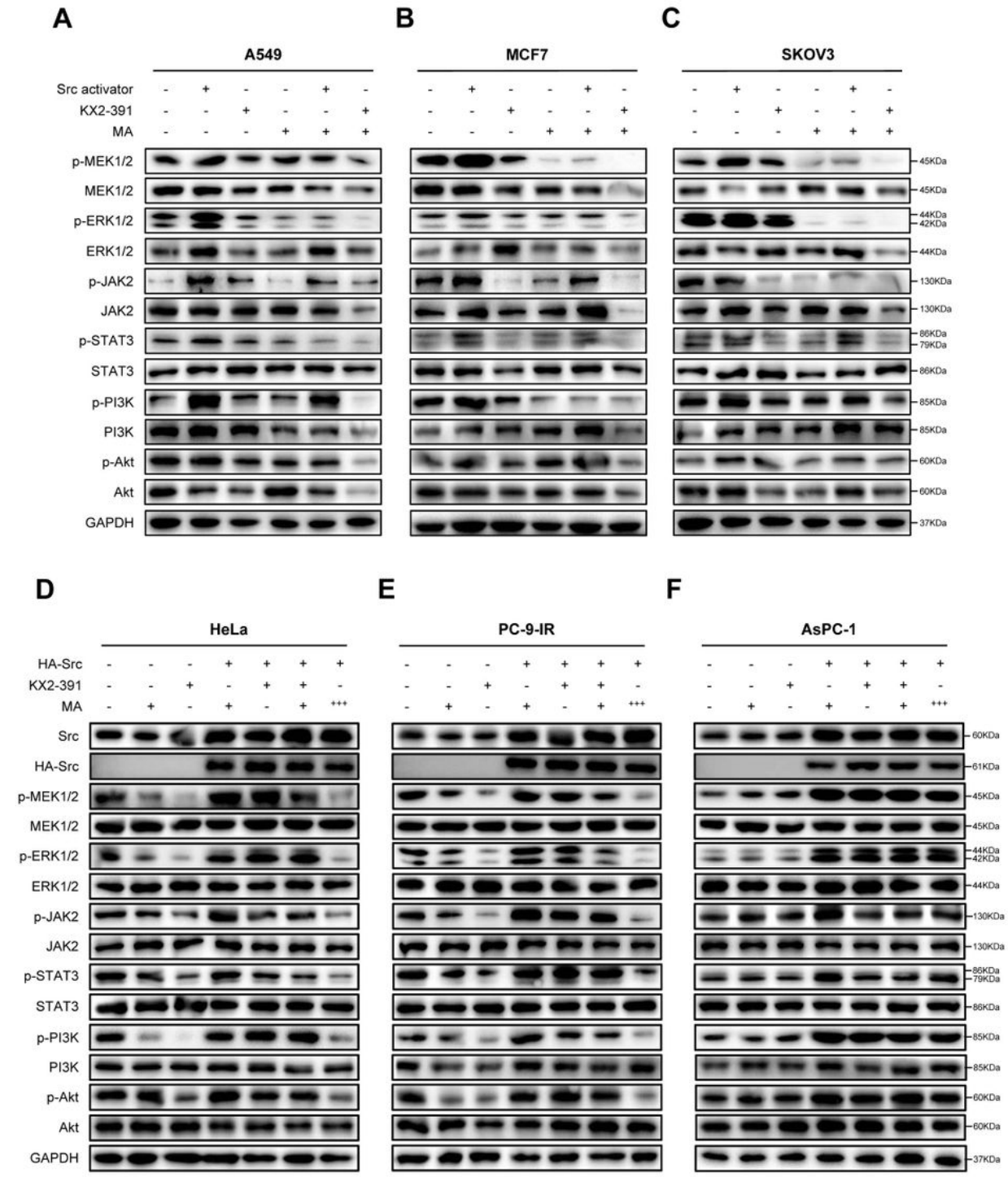

Figure 6

Involvement of Src in matrine-mediated phosphorylation signaling pathways. a-c A549, MCF7 and SKOV3 cells were treated with Src activator or Src inhibitor KX2-391, then exposed to matrine at its optimal concentrations for 24 h, respectively. The phosphorylation levels of MAPK/ERK, JAK2/STAT3 and PI3K/Akt signaling pathways in A549 (a), MCF7 (b) and SKOV3 (c) cells were examined, respectively. d-f Human cervical cancer cell HeLa, gefitinib-resistant human lung cancer cell PC-9-IR and human pancreatic cancer cell AsPC-1 were transfected with plasmid pcDNA3.1-HA-Src, then treated with matrine, KX2-391 and excessive matrine, respectively. The phosphorylation levels of MEK1/2, ERK1/2, JAK2, STAT3, PI3K and Akt in HeLa (d), PC-9-IR (e) and AsPC-1 (f) were detected by Western blot, respectively. GAPDH was used as control.

Fig.7

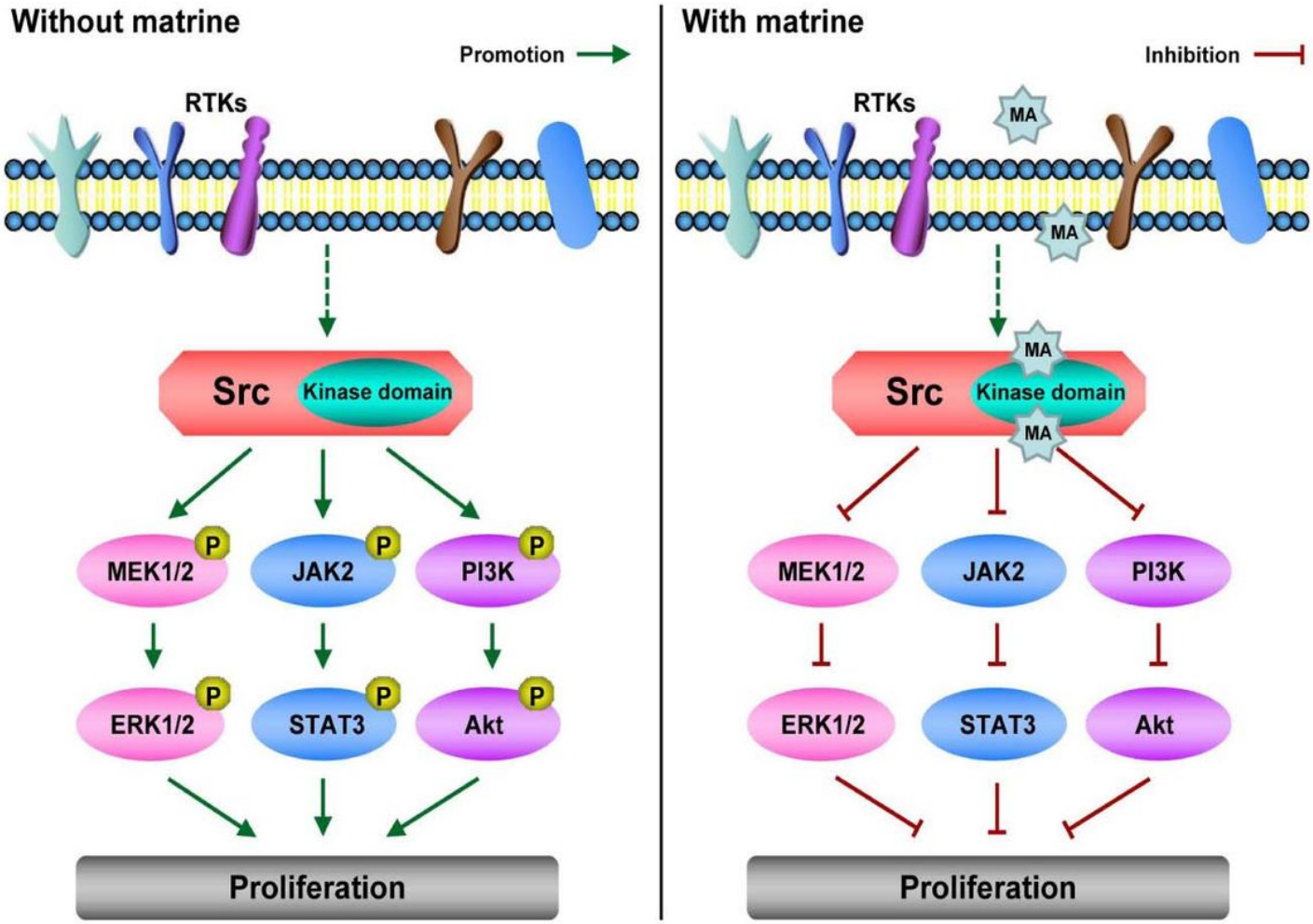

Figure 7

Schematic diagram of matrine inhibiting the proliferation of cancer cells.

Fig.7

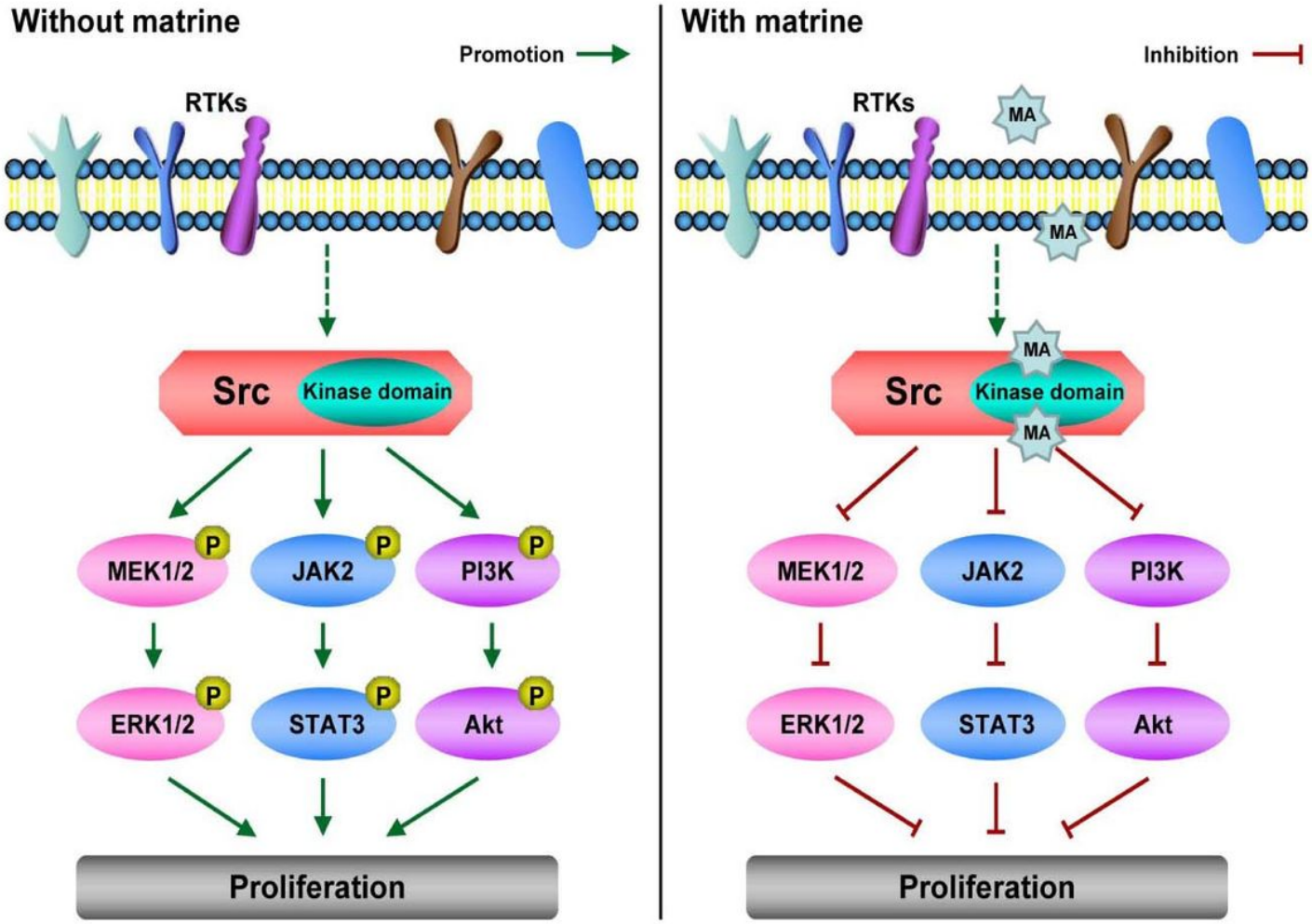

Figure 7

Schematic diagram of matrine inhibiting the proliferation of cancer cells.

Fig.7

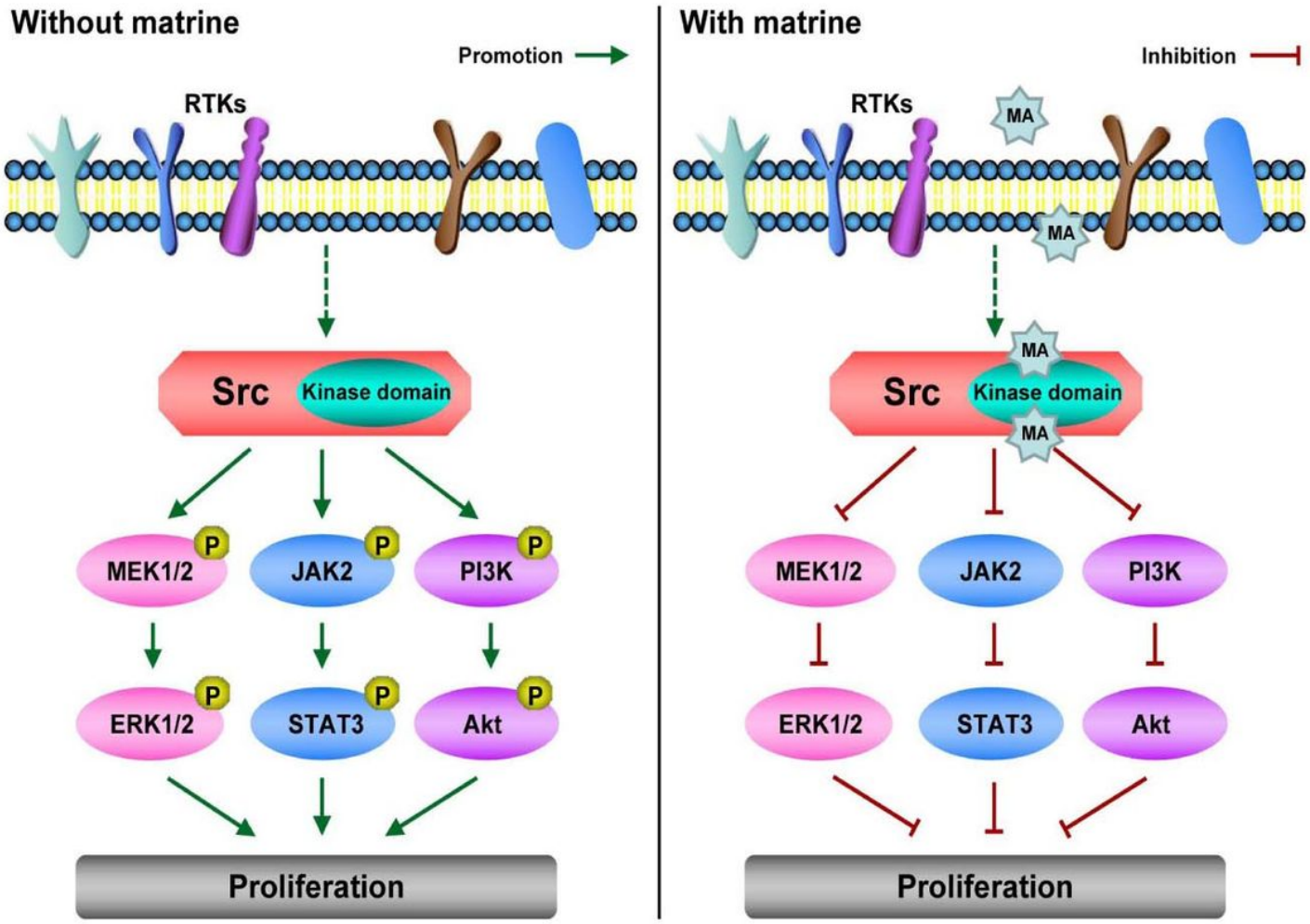

Figure 7

Schematic diagram of matrine inhibiting the proliferation of cancer cells.

Supplementary Files

This is a list of supplementary files associated with this preprint. Click to download.

- Fig.S1.jpg
- Fig.S1.jpg
- Fig.S1.jpg
- Fig.S2.jpg
- Fig.S2.jpg

- Fig.S2.jpg
- Fig.S3.jpg
- Fig.S3.jpg
- Fig.S3.jpg
- Fig.S4.jpg
- Fig.S4.jpg
- Fig.S4.jpg
- Fig.S5.jpg
- Fig.S5.jpg
- Fig.S5.jpg
- TableS1.doc
- TableS1.doc
- TableS1.doc
- TableS2.doc
- TableS2.doc
- TableS2.doc
- TableS3.doc
- TableS3.doc
- TableS3.doc